PNC-TN960 79-04

高速炉燃料挙動に関する国際会議(モントレー会議)

海外出張報告書

1979年6月

動力炉・核燃料開発事業団

動力炉・核燃料開発事業団（Power Reactor and Nuclear Fuel Development Corporation）

PNC-TN960 79-04
1 9 7 9 年 6 月

高速炉燃料挙動に関する国際会議(モントレー会議)

海 外 出 張 報 告 書

河 田 東海夫 * 永 井 寛 **

要 旨

1979年3月5日から3月8日まで4日間，米国カリフォルニア州モントレーで米国原子力学会（ANS）主催の高速炉燃料の照射挙動に関する国際会議（International Conference on Fast Breeder Reactor Fuel Performance）が開催された。

この会議には，米国をはじめ各国から約200名の参加者があり，80件の論文発表，討論が行なわれた。動燃事業団からは，筆者ら2名が参加し2件の論文を発表した。

本報告書では，会議の概要を整理するとともに筆者らの発表内容を添付した。

* 大洗工学センター燃料材料試験部照射燃料試験室（現在 高速増殖炉開発本部）

** 大洗工学センター燃料材料試験部照射燃料集合体試験室

目　　次

1　モントレー会議の概要

1979年3月5日から4日間，米国カリフォルニア州モントレーで米国原子力学会（ANS）主催の高速炉燃料の照射挙動に関する国際会議が以下のような日程で開催された。

会　議　日　程　概　略

3月5日（月）	Session Ⅰ；酸化物燃料の照射挙動
3月6日（火）	Session Ⅱ；燃料挙動とそのメカニズム，熱的特性， ＦＰ挙動，燃料／被覆管相互作用他 （午前　口答発表，午後　ポスターセッション）
3月7日（水）	Session Ⅲ；燃料設計（含集合体設計）とモデリング
3月8日（木）	Session Ⅳ；新型，および代替燃料
	Session Ⅴ；パネル・ディスカッション（15：30～16：30）

この会議では，米国をはじめとする各国から，第2日目午後のポスター・セッションでの発表を含めると合計80件の最新論文が紹介された。

国　別　発　表　件　数

米　国	西　独	英　国	フランス	日　本	その他	合　計
41	13	9	8	4	5	80

会議のプログラム詳細と参加者（約200名）の名簿を5～9ページに示した。会議で発表された論文はすべてProceeding（ISBN：O－89448－105－3，International Conference on Fast Breeder Reactor Fuel Performance）に収録されているので，内容に興味のある方はこれを直接御参照されたい。（本社技術情報室に1冊，東海Ｐｕ燃部に1冊，大洗燃材部に2冊分置）

なお，内容の概略をいくつかのテーマ別に分類して附録－1にまとめた。またこの会議における筆者らの発表内容を附録－2，および附録－3に添付した。

＊　　＊　　＊

モントレー会議に引続いて，3月12日から14日までの3日間HEDL（Hanford Engineering Development Laboratory）で燃料ピン照射データに関する日米燃材専門家会議が開催され，筆者らがこれに参加した。会議のテーマには「高燃焼度照射ピンに関するデータ」，「ピン破損経

験」等が含まれており，モントレー会議における日米の発表内容を，具体的なデータで補足するかたちの会議となった。この会議の概要については，別報告書（PNC SN960 79−05 ；海外出張報告：高速炉用燃料照射データに関する日米燃材専門家会議）にまとめたので，興味のある方は御参照戴きたい。

2　高速炉用燃料の照射挙動

モントレー会議における各国からの発表内容をもとに高速炉燃料の照射挙動についての今日までの知見を何点かについて総括してみると，以下のようになる。

A　燃料ピンの照射挙動

① 各国ともに燃料ピン照射実験で10 atom％（～100,000 MWD／MTM）を超える燃焼度，10^{23} nvtを超える高速中性子フルエンスを得ている。

② 現在の316ステンレス鋼系の被覆管を使う限り，高フルエンス下での燃料ピンの直径増加は相当大きくなる。（1.2×10^{23} nvtで　$\Delta D_{max}/D = 2\sim10$％，Fig. 1参照）
直径増加の主要原因は被覆管のスウェリングと照射クリープ。

③ 被覆管の内面腐食（FCCI）は，実効肉厚減少に寄与するが，燃料ピン寿命制約の第一義的要因とはならない。

④ 燃料・被覆管機械的相互作用（FCMI）は，それが発生しても定常照射下では特に問題となることはない。但し，定常時FCMIが発生している時に急激な出力上昇やTOPが重なると被覆管に大きな損傷を与える可能性がある。

⑤ 典型的なFBR使用条件のもとで，15 atom％以下の燃焼度では被覆管クリープ寿命の消耗によるピン破損は生じていない。

⑥ ②～⑤から，現在のところ燃料ピンの実際的な使用限界を決める最大の要因は，高フルエンスにおける被覆管のスウェリングおよび照射クリープによる直径増加（Fig. 1参照）と考えられる。

⑦ 各国が経験しているピン破損の大半は（ピン曲がり，気泡附着等による）局所過熱が原因。

⑧ ピン破損伝播は，ほとんどの場合起らない。

B　集合体の照射挙動

① すきまの多い構造のピン束の場合，振動摩擦により被覆管肉厚がすり減ることがあり，一方きつい構造のピン束では高フルエンス下で，ピン束／ラッパ一管相互作用が生ずる。これまでの経験（EBR－Ⅱ，ラプソディ）からすると，若干のピン束／ラッパ一管相互作用は実用上許容できそうである。

② 原型炉クラスの炉も含め，大型炉では高フルエンス下でのラッパ一管の変形（ふくれ，曲がり）が燃料交換機の機能との関連で重要。ラッパ一管変形による集合体の使用限界は，ピンのふくれ，またはピン束／ラッパ一管相互作用による使用限界と競合し，実質的には前者によって使用限界が決まる可能性が大きい（Phenixの例）。

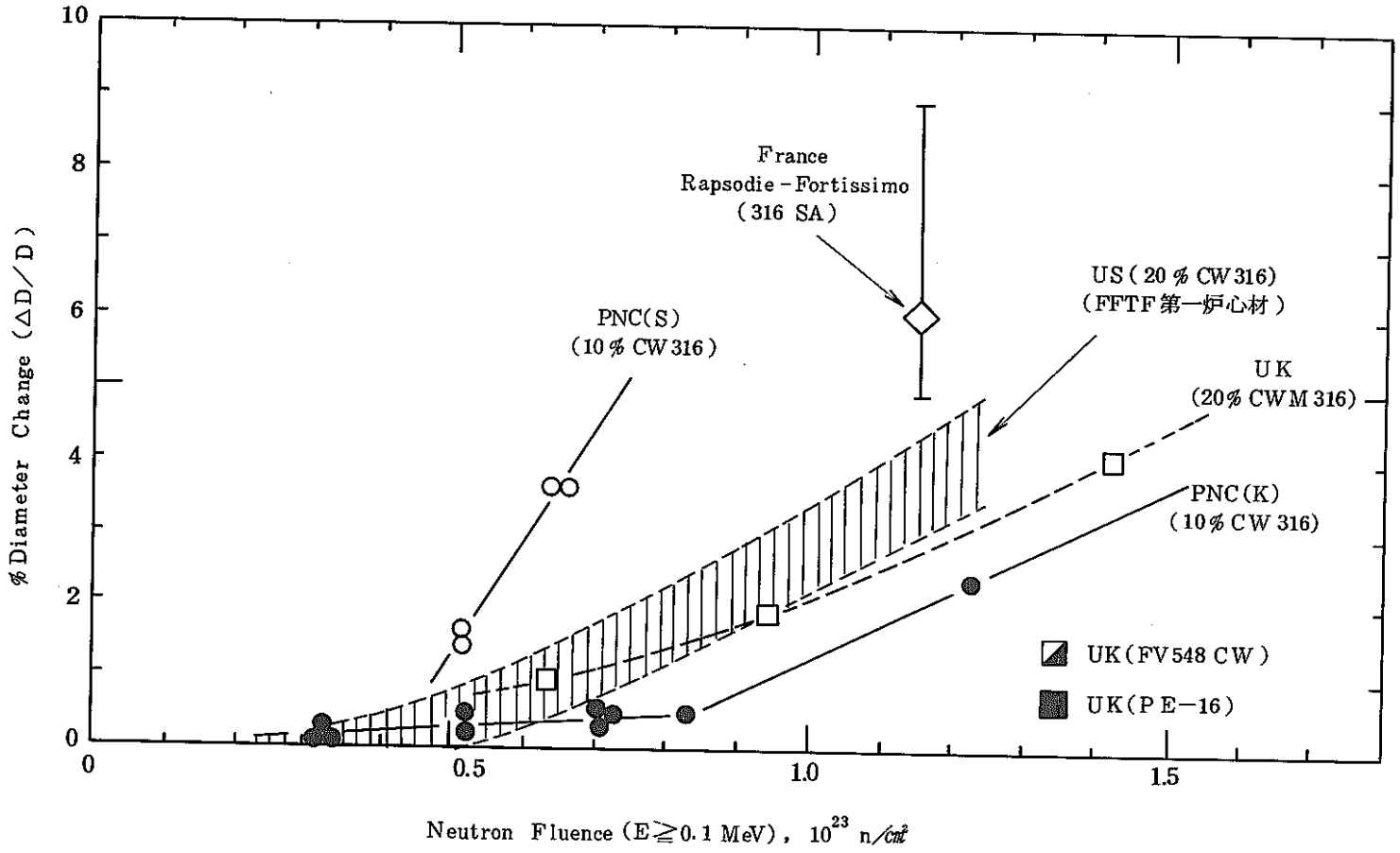

Fig. 1　高フルエンスにおける燃料ピン外径変化（各国の実績比較）

3 会 議 目 録

International Conference on Fast Breeder Reactor Fuel Performance

Cosponsored by American Nuclear Society, Materials Science Technology Division, Fuel Cycle Division, and San Francisco Section; by the Nuclear Metallurgy Committee of The Metallurgical Society, AIME; and by U.S. Department of Energy

Monterey Conference Center
Monterey, California
March 5-8, 1979

This meeting is intended to serve as a broadly-scoped international conference that will focus on breeder reactor fuel performance. The sessions offer an opportunity to exchange technical information on the design, testing and operation of fast reactor fuel assemblies and to assess the current status and direction of development programs. The meeting will feature invited papers, contributed papers, poster session, and panel discussion. Topics included are: (1) mixed oxide fuel irradiation performance; (2) properties and mechanisms including thermal, mechanical and transport properties, fuel chemistry and fission product behavior, fuel-cladding interactions, and fuel-coolant interactions; (3) fuel design and modeling; and (4) advanced and alternative fuels.

PROGRAM

Monday, March 5

Welcoming Remarks:
E.A. Aitken, General Chairman ..... 8:25 A.M.

Keynote Speaker:
R.L. Ferguson, Prog. Dir. for Nuclear Energy ..... 8:30 A.M.

SESSION IA. MIXED OXIDE FUEL IRRADIATION PERFORMANCE ..... 9:15 A.M.-12:30 P.M.

① **Steady-State Irradiation Behavior of Mixed Oxide Fuel Pins Irradiated in EBR-II**, R.D. Leggett, E.N. Heck, P.J. Levine, and R.F. Hilbert (USA)

② **Irradiation Performance of Mixed Oxide Fuel Pins — Japanese Experience**, K. Uematsu, Y. Ishida, J. Komatsu, and T. Kawada (Japan)

③ **The German Oxide Fuel Pin Irradiation Test Experience for Fast Reactors**, K.R. Kummerer (Germany)

④ **Prediction and Follow Up of the Behavior of Fuel Subassemblies and of Experimental Irradiation in the PHENIX Breeder**, P. Coulon, M. Carnoy and P. Courcon (France)

⑤ **Mixed Oxide Fuel Performance**, E. Edmonds, W. Sloss, K.Q. Bagley, W. Batey (UK)

⑥ **Irradiation Experiments in the Development of a Vented Helium-Cooled Fast Breeder Reactor Fuel Design**, J.R. Lindgren, S. Langer, R.J. Campana, R.T. Acharya, P.W. Flynn, G. Buzzelli, S. Greenberg and A.W. Longest (USA)

⑦ **Irradiation of GCFR Test Fuel Bundles in the BR-2 He-Loop-MOL**, W. Krug, H. Euringer, W. Jung, C. Vanmassenhove, and R.J. Campana (Germany)

SESSION IB. MIXED OXIDE FUEL IRRADIATION PERFORMANCE ..... 2:00-5:10 P.M.

⑧ **HEDL Mixed Oxide Fuel Pin Breach Experience in EBR-II**, J.W. Weber, M.Y. Almassy, and R.A. Karnesky (USA)

⑨ **Mixed Oxide Run-Beyond-Cladding-Breach Tests in EBR-II**, D.F. Washburn, M.Y. Almassy, D.C. Langstaff, J.D.B. Lambert, and R.V. Strain (USA)

⑩ **Defect Pin Behavior in the DFR**, W.M. Sloss, K.Q. Bagley, E. Edmonds, and P.E. Potter (UK)

⑪ **Cladding Deformations in Rapsodie and Their Consequences**, G. Marbach, P. Millet, and R. Peray (France)

⑫ **Aspects of the Restructuring of Oxide Fuel**, R. Paris, J.M. Horspool and G.R. Bellamy (UK)

⑬ **Irradiation Performance of WSA-3, -4, and -6 Mixed Oxide Fuel Pins in Grid-Spaced Assemblies**, P.J. Levine, U.P. Nayak, A.L. Schwallie, and A. Boltax (USA)

⑭ **Fast Reactor Fuel Pin Performance Requirements for Off-Normal Events**, R.E. Baars, T. Hikido, and J.E. Hanson (USA)

Tuesday, March 6

SESSION IIA. PROPERTIES AND MECHANISMS ..... 8:30-11:40 A.M.

⑮ **Swelling, Densification and Creep of Oxide and Carbide Fuels Under Irradiation**, W. Dienst, I. Mueller-Lyda, and H. Zimmermann (Germany)

⑯ **The Development of Physical Models for Fission Gas Behavior in Nuclear Fuels Under Operational and Transient Conditions**, M.R. Hayns and M.H. Wood (UK)

⑰ **Thermochemical Data and Its Use in Modeling Chemical Behavior in Mixed Oxide Fuel Pins**, R.L. Gibby, R.E. Woodley, M.G. Adamson, and C.E. Johnson (USA)

⑱ **Diffusion Based Phenomena in Fast Breeder Fuel Materials**, Hj. Matzke (Germany)

⑲ **Development and Testing of a Physicochemical Model for Prediction of Reaction Swelling in Breached Oxide Fuel and Breeder Elements**, R.W. Caputi, M.G. Adamson, and S.K. Evans (USA)

⑳ **Fuel/Clad Reactions in Mixed Oxide Fuel Pins**, K.Q. Bagley, W. Batey, J.R. Findlay, and R. Paris (UK)

㉑ **Fuel-Cladding Mechanical Interaction-Observations and Analysis**, J.P. Gatesoupe, Y. Guerin, C. Courtois and J. Truffert (France)

SESSION IIB. POSTER SESSION ..... 2:00-5:00 P.M.

Section A. Thermal, Mechanical and Transport Properties

㉒ **Early-in-Life Thermal Performance of UO_2-PuO_2 Fast Reactor Fuel**, R.B. Baker and R.D. Leggett (USA)

㉓ **The Influence of Design and Operating Parameters on Mixed-Oxide Fuel Power-to-Melt**, W. McCarthy, D.R. Jedlovec, S. Vaidyanathan, and R.F. Hilbert (USA)

㉔ **Material Transport Processes and Their Effects in Fast Breeder Mixed Oxide Fuel**, G. Schumacher (Germany)

㉕ **Application of a Cluster Model of Oxygen Thermomigration to Fast Reactor Fuel Behavior**, D.I.R. Norris, K.A. Simpson (UK)

㉖ **Study of the Thermal Behavior of LMFBR Fuel**, M. Conte, J.P. Gatesoupe, M. Trotabas, J.C. Boivineau and G. Cosoli (France/Italy)

㉗ **Behavior of Irradiated UO_2-PuO_2 Under Simulated Cyclic Overpower Transients**, G.L. Hofman, G. Bandyopadhyay, F.L. Brown and J.A. Buzzell (USA)

㉘ **Behavior of Pellet and Particulate Oxide Fuel During Simulated and Multiple Overpower Transients**, J.H. Bottcher, J.A. Buzzell and G.L. Hofman (USA)

㉙ **Swelling in Advanced Fuels up to High Heat Ratings**, H. Blank and Hj. Matzke (Germany)

㉚ **Initial Stage Restructuring in Sphere-Pac Mixed Carbide Fuel**, R.J. Guenther and K.L. Peddicord (USA)

Tuesday, March 6 (continued)

Section B. Fission Product Behavior and Chemistry

31. **Cesium Migration in LMFBR Fuel Pins**, R.A. Karnesky, J.W. Jost, and I.Z. Stone (USA)
32. **Fission Product Release and Transport in GCFR Sealed and Vented Irradiation Experiments**, S. Langer, G. Buzzelli, J.R. Lindgren, P.W. Flynn, R.J. Campana, L.A. Neimark, S. Greenberg and C.E. Johnson (USA)
33. **Cesium Chemistry in GCFR Fuel Pins**, D.C. Fee and C.E. Johnson (USA)
34. **Migration Behavior of Cesium in Mixed Oxide Fuel Pins**, K. Uematsu, Y. Ishida, J. Komatsu, and T. Kawata (Japan)
35. **The Chemical State of Irradiated Uranium-Plutonium Oxide Fuel Pins**, H. Kleykamp (Germany)
36. **Fission Gas Behavior in Mixed Oxide Fuel During Overpower and Thermal Transient Tests**, E.H. Randklev and C.A. Hinman (USA)
37. **Modeling of Isotopic Fission Gas Release in the GCFR Vented Fuel Rod**, K.H. Chang, M.P. LaBar, and R.J. Campana (USA)

Section C. Fuel-Cladding Interaction

38. **Fuel-Cladding Chemical Interaction in Mixed-Oxide Fuels**, L.A. Lawrence, J.W. Weber, and J.L. Devary (USA)
39. **In Reactor Performance of Methods to Control Fuel-Cladding Chemical Interaction**, E.T. Weber, R.L. Gibby, C.N. Wilson, L.A. Lawrence and M.G. Adamson (USA)
40. **The Effect of Fuel Density on Fuel-Cladding Mechanical Interaction**, S. Vaidyanathan, and R.F. Hilbert (USA)
41. **A Review of Examinations and Considerations on Cladding Distension by Mechanical Interaction with the Fuel in Fast Breeder Fuel Pins**, W. Dienst and I. Mueller-Lyda (Germany)
42. **Fuel Adjacency Effects on Fast Reactor Cladding Mechanical Properties**, C.W. Hunter and G.D. Johnson (USA)
43. **A Thermochemical Model for Fuel-Cladding Chemical Interactions in Oxide Fuel Pins**, O. Goetzmann (Germany)
44. **In-Pile Simulation of Fuel-Cladding Interaction**, A. Delbrassine (Belgium)
45. **Techniques for Studying Inner Cladding Corrosions in Irradiated LMFBR Pins**, M. Coquerelle, S. Pickering, I.L.F. Ray, C.T. Walker, and W.H. Whitlow (Germany)
46. **Fuel-Cladding Mechanical Interaction in Fast Reactor Fuel Rods**, A. Biancheria, T.S. Roth, U.P. Nayak, and A. Boltax (USA)
47. **Mechanism and Prediction of FCCI in Mixed-Oxide Fuel Pins at High Burnup: Evidence for Cladding Component Chemical Transport**, M.G. Adamson and E.A. Aitken (USA)
48. **Fuel-Cladding Mechanical Interaction in Irradiated GCFR Mixed-Oxide Fuel Rods**, K.H. Chang and M.P. LaBar (USA)
49. **An Analysis of Mechanical Interaction Between Fuel Pellets and Cladding**, M. Ishida, M. Sakagami, and S. Kikuchi (Japan)
50. **Statistical Analysis and Parameter Study of Chemical Fuel/Cladding Interaction of SNR-Typical Fast Flux Experiments**, W.K. Biermann, D. Haas and H.J. Heuvel (Germany)
51. **Some Observations on the Carburization of Mixed Oxide Pin Clad in the Dounreay Fast Reactor**, R.G. Bellamy and R. Paris (UK)

Section D. Fuel Pin-Coolant Interactions

52. **Distribution of Fission Products Released from Breached Mixed-Oxide, -Carbide, -Nitride, and Metallic Fuels Irradiated in EBR-II**, R. Villarreal (USA)
53. **Analysis of Fission Product Release from Vented LMFBR Fuel Pins**, P. Cecchi and G. Scandola (Italy)
54. **Release of Fission Products from Artificially Defected LMFBR Oxide Fuel Pins**, S. Jacobi and G. Schmitz (Germany)

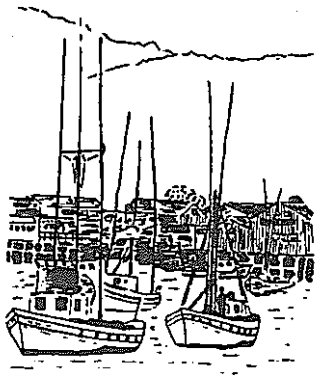

Wednesday, March 7

SESSION IIIA. FUEL DESIGN AND MODELING . . . . . 8:30 A.M.-12:15 P.M.

Section A. Fuel Pin Modeling

55. **Evaluation of Fast Breeder Reactor Fuel Pin Performance During Normal Operation**, B.L. Harbourne, M.R. Patel, J.D. Stephen, B.E. Sundquist, M.C. Billone, D.S. Dutt, and B.J. Ostermeier (USA)
56. **Modeling of Fast Reactor Fuel Transient Behavior Using the LIFE Code**, T.S. Roth, D.B. Atcheson, A. Biancheria, M.C. Billone, J.D. Stephen, and B.E. Sundquist (USA)
57. **LMFBR Fuel Pin Modeling with the Computer Codes COMETHE III J and IAMBUS**, J. Van Vliet, A. Pay, H. Tobbe and B. Steinmetz (Germany/Belgium)
58. **FRUMP — A Physically Based Model**, D. Wilmore and J.R. Mathews (UK)
59. **An Evaluation of FBR Irradiation Behavior Using a Hybrid Computer**, T. Ishii, M. Mizuno, and T. Kubota (Japan)
60. **Probabilistic Methods for LMFBR Application**, D.S. Dutt, K.H. Chen, J.D. Stephen and B.D. O'Reilly (USA)

Section B. Fuel Assembly Design and Experience

61. **Experimental Fuel Subassembly Irradiation Experience in EBR-II**, R.J. Jackson, S. Kaplan, and A.L. Schwallie (USA)
62. **Design and Performance Improvements of Commercial Fast Reactor Subassemblies Using PHENIX Experience**, G. Arnaud, A. Bernard, J.M. Dupouy and J.L. Boutard (France)

SESSION IIIB. FUEL DESIGN AND MODELING . . . . . 2:00-5:15 P.M.

Section C. Fuel Pin and Assembly Design Units and Criteria

63. **Fuel Pin and Assembly Design Limits and Criteria**, R.M. Vijuk, D.S. Dutt, and J.D. Stephen (USA)
64. **Problems Encountered in the Design of Fuel Elements for Fast Breeder Reactors — Solutions Taken Up in France**, J. Leclere (France)
65. **Aspects of LMFBR Oxide and Carbide Fuel Element Design and Analysis with Respect to Thermodynamic and Fluidynamic Optimized Grid and Wire-Spaced Assemblies**, H. Hoffmann and D. Weinberg (Germany)

Section D. Advanced Fuel Assembly Design

66. **Summary of Advanced Concepts in Fuel Assembly Design**, S. Kaplan, J.D. Stephen, R.M. Vijuk, and R.J. Jackson (USA)
67. **Fast Neutron Reactor Fuel Elements: Power Grid Duty Problems**, J. Rousseau, A. Chalony, C. Acket, and J. Decuyper (France)
68. **Advanced Subassembly Design for CDFR**, J.A. Gatley (UK)

Thursday, March 8

SESSION IVA. ADVANCED AND ALTERNATIVE FUELS . . . . . 8:30-12:05 P.M.

69. **Advanced/Alternate Breeder Fuels Testing in the U.S.**, J.W. Bennett, E.C. Norman, C.M. Cox, M.G. Adamson, A. Boltax and J.H. Kittel
70. **Design and Performance of Sodium-Bonded Uranium-Plutonium Carbide Fuels**, J.F. Kerrisk, N.S. DeMuth, R.L. Petty, T.W. Latimer, J.A. Vitti, and L.J. Jones (USA)
71. **Irradiation Performance of Helium-Bonded Uranium-Plutonium Carbide Fuel Elements**, T.W. Latimer, R.L. Petty, J.F. Kerrisk, N.S. DeMuth, P.J. Levine and A. Boltax (USA)
72. **He- and Na-Bonded Mixed-Nitride Fuel Performance**, A.A. Bauer, P. Cybulskis, N.S. De Muth and R.L. Patty (USA)
73. **Performance Analysis of Helium-Bonded Carbide and Nitride Fuel Pins**, A. Boltax, U.P. Nayak, R.J. Skalka, and A. Biancheria (USA)
74. **Behavior of Advanced Carbide Fuel During Transient Overpower Operations**, H.C. Tsai, L.A. Neimark and D.L. Johnson (USA)
75. **The Performance of EBR-II Mark-II Metallic Driver Fuel up to 675°C**, R.E. Einziger (USA)

SESSION IVB. ADVANCED AND ALTERNATIVE FUELS . . . . 1:30-3:35 P.M.

76. **The Performance of FBR Core Designs with Alternative Fuel**, C.E. Weber, V.W. Lowery, A. Biancheria, and R.P. Omberg (USA)
77. **Design of Carbide Fueled LMFBR Cores**, R.C. Noyes, R.H. Klinetob, and M.R. Kulwich (USA)
78. **Optimization of a Carbide Element for Low Doubling Time**, J.C. Mougniot, J. Recolin, M. Colin, and J. Rouault (France)
79. **Metallic Fuels Systems for Alternative Breeder Fuel Cycles**, J.H. Kittel, D.L. Johnson, W.N. Beck, and J.A. Horak (USA)
80. **Performance of U-Pu-Zr Metal Fuel in 1000 MWe LMFBRs**, P.S.K. Lam, R.B. Turski and W.P. Barthold (USA)

SESSION V. PANEL DISCUSSION . . . . . 4:00-6:00 P.M.

4 会議出席者名簿

ANS FAST BREEDER REACTOR CONFERENCE ATTENDEES AS OF 3/5/79

W. K. Appleby, GE
E. A. Aitken, GE
M. G. Adamson, GE
E. J. Aitken, Oregon State
G. Arnaud, CEA
D. B. Atcheson, GE

T. H. Brown, LASL
J. P. Bacca, ANL-Idaho
R. B. Baker, HEDL
J. Bottcher, ANL
H. Blank, Transuranium Elements, Karlsruhe
B. W. Bremer, CE
R. G. Bellamy, UKAEA
J. Boutard, CEA
W. P. Barthold
A. Biancheria, WARD
G. Bandyopadhyay, ANL
H. S. Bailey, GE
A. Boltax, WARD
R. G. Ballinger, MIT
F. Botta, Swiss FIRR

R. J. Campana, GA
J. P. Colton, IAEA, Vienna
C. M. Cox, HEDL
S. A. Casperson, CE
P. Coulon, CEA
P. Cybulskis, Battelle
M. M. Cornu, Ed-F-REAL
R. W. Caputi, GE
W. D. Craig, GE
D. Croucher, EG&G
K. H. Chang, GA
A. Calza-Bini, CNEN-CEN
R. Colburn, HEDL
C. Cole, GE

L. W. Dietrich, ANL-East
W. Dienst, KFD, Karlsruhe
D. S. Dutt, HEDL
B. D'Onghia, NERSA
Decuyper, NERSA
D. de Herring, Belgonucleaire, Belgium
N. S. Demuth, LASL
E. Duncombe, B.E.P.
A. Delbrassine, CEN/SCK, Belgium

E. A. Evans, HEDL
R. Einziger, ANL, Idaho
D. Eldred, GE
H. Euringer, KFA
E. Edmonds, UKAEA

D. Fee, ANL
E. M. Franklin, ANL, Idaho
G. R. Fenski, ANL-East
L. D. Felton, AI
E. L. Fuller, EPRI
J. R. Findley, UKAEA

S. Goldsmith, Battelle
O. Goetzmann, KFK
A. Gloaguen, Electricite de France
F. Grigon, COGEMA
R. Guenther, Oregon State
J. P. Gatesoupe, CEA
Y. Guerin, CEA
P. Gross, DOE-CRBRP
T. Guo, People's Republic of China
K. Gregoire, GE

T. Hikido, HEDL
G. L. Hofman, ANL-East
J. M. Horspool, UKAEA
F. J. Homan, ORNL
H. Heuvel, Interatom
H. Hayashi, FBR Engrng. Office
B. L. Harbourne, GE
C. Hunter, HEDL
W. Hongion, People's Republic of China
H. Hoffman, KFK
R. F. Hilbert, GE
W. Henoch, DOE
J. E. Hanson, HEDL

M. Ishida, Hitashi

C. E. Johnson, ANL-East
R. J. Jackson, HEDL
L. J. Jones, AI
F. Jonsson, Studsvik

H. Kleykamp, KFK
K. R. Kummerer, KFK
R. A. Karnesky, HEDL
R. H. Klinetob, CE
T. Kawata, PNC
D. L. Keller, Battelle Off. Nucl. Waste
J. J. Krupar, DOE/FFTF
J. H. Kittel, ANL
V. Keshishian, AI
J. Keating, DOE/FFTF
D. Kaulitz, HEDL

L. A. Lawrence, HEDL
R. D. Leggett, HEDL
R. J. Loyd, EG&G
J. R. Lindgren, GA
T. B. Lanahan, FMC
J.D.B. Lambert, ANL-East
T. Lindemer, ORNL
T. Latimer, LASL
M. La Bar, GA
J. J. Laidler, HEDL
S. Langer, GA
E. L. Long, ORNL
L. Lincoln, GE

P. K. Mast, LASL
G. C. McClellan, ANL
L. C. Michels, LASL
M. Mustelier, COGEMA
H. Matzke, EURATOM
F. McCuaig, ANL-East
A. J. McSherry, GE
W. H. McCarthy, GE
J. Marcon, CEA
D. E. Mahagin, HEDL
P. Millet, CEA
J. M. Morelle, INB
Xu Mi, People's Republic of China
M. Mizuno, Mitsubishi
A. Marshall, Sandia Labs

F. A. Nichols, ANL
L. A. Neimark, ANL
H. Nagai, PNC
E. C. Norman, DOE

B. J. Ostermier, Rockwell Intnl.

K. L. Peddicord, Oregon State Univ.
D. E. Plumlee, GE
R. L. Petty, LASL
R. Pascard, CEA

E. H. Rankklev, HEDL
F. Robert, NOVATOME
J. M. Rosa, GE
J. Rousseau, CEA
J. Recoulin, CEA
R. B. Richard, GE

J. H. Scott, LASL
G. Schmitz, KFK
G. Schumacher, KFK
D. L. Selby, ORNL
B. Steinmitz, INTERATOM
J. A. Shields, ANL-Idaho
B. R. Seidel, ANL-Idaho
M. T. Simnad, GA
B.Y.C. So, ANL-East
V. W. Storhok, EG&G
J. S. Salmon, UKAEA
J. Simmons
J. D. Stephen, GE
W. Sloss, UKAEA
A. Solomon, Purdue Univ.
R. Staker, GE

H. C. Tsai, ANL-East
K. Ting, ANL-East

J. Usselman, GE

R. Villereal, ANL-East
R. M. Vijuk, WARD
S. Vaidyanathan, GE
K. Van Vliet, Belgonucleaire
A. R. Veca, GA

T. R. Wehner, LASL
D. F. Washburn, HEDL
J. W. Weber, HEDL
W. L. Wang, ANL-East
B. J. Wrona, Babcock & Wilcox
L. G. Williams, UK Nuclear Inspectorate
A. R. Wazzan, UCLA
W. B. Wolfe, AI
E. T. Weber, HEDL

S. T. Yang, UC Berkeley
T. Yokoyama, Toshiba
A. Yee, HEDL

B. Zhou, People's Republic of China

附録－1

モントレー会議文献抜萃

モントレー会議発表内容を以下のようなテーマ別に分類してまとめた。○で囲んだ数字は，会議目録に附した文献番号を示す。

1. 高フルエンス下での燃料ピン外径変化
2. 燃料ピンの使用限界，破損経験
3. 破損燃料ピンの継続照射
4. 燃料の熱的挙動
5. ＦＰガス放出率
6. ＦＣＭＩ（Fuel－Cladding Mechamical Interaction）
7. ＦＣＣＩ（Fuel－Cladding Chemical Interaction）
8. Csの軸方向移行
9. 集合体としての高燃焼度照射実績
10. ピン束振動及びピン束／ラッパー管相互作用
11. 燃料ピン挙動のモデリング
12. 新型および代替燃料（米国）

1　高フルエンス下での燃料ピン外径変化（max△D/D）

米　　国　　①

○ FFTF 第１炉心用被覆管を使用した燃料ピン照射（ in EBR－Ⅱ）

$(\phi t)_{fast} = 1.2 \times 10^{23}$ nvt で

max △D/D＝3.2 ～ 4.7 %

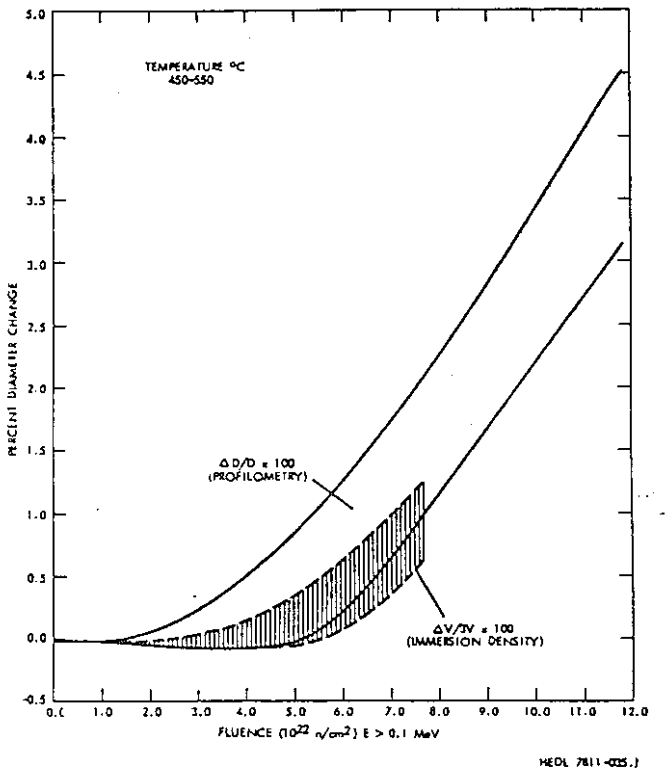

Figure 3.　Diameter Change for Fuel Pins Clad with Core 1 Steel (316 20% CW) and Irradiated in EBR-II.

英　　国　　⑤

○ ３種類の被覆管を使用した燃料ピン照射実験（ＤＦＲ）

B. U.　　＝ 17.2 atom%

$(\phi t)_{fast} = 1.43 \times 10^{23}$ nvt

被 覆 材	max△D/D (%)
M316（20%CW）	4.1
FV548（20%CW）	1.2
PE－16（ST）	0.4

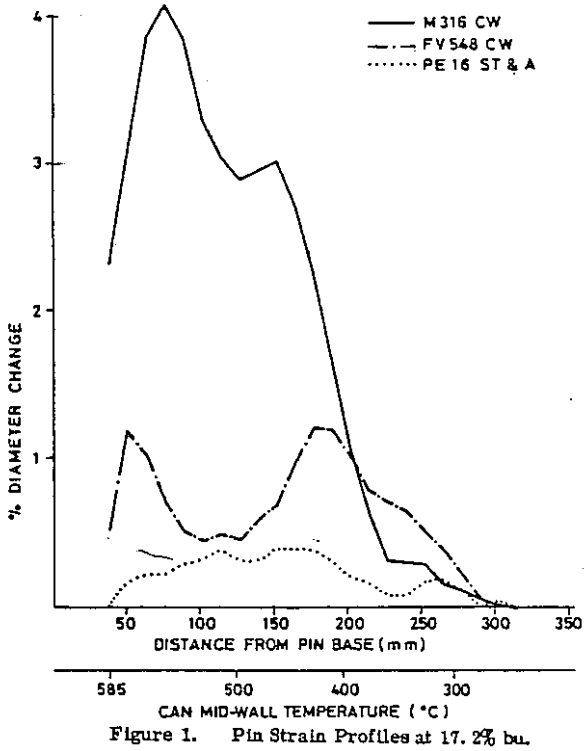

Figure 1.　Pin Strain Profiles at 17.2% bu.

フランス　⑪

○ラプソディ・フォルティシモの標準ドライバー燃料S／Aの燃料ピン径変化

Subassembly 59　　B．U＝13 at％

（clad＝316 S.A.）　（ϕt）$_{fast}$ ＝ 1.15×10^{23} (77 dpa)

max△D/Dの平均 ≒ 6 ％

S／A内側ピン　　5 ～ 9 ％（Single peak）

S／A外周ピン　　3 ～ 5 ％（double peak）

（△D／Dが燃料カラムをはずれたところで急に落ちこまない点が冷間加工材を使っている他の国の例と異る。）

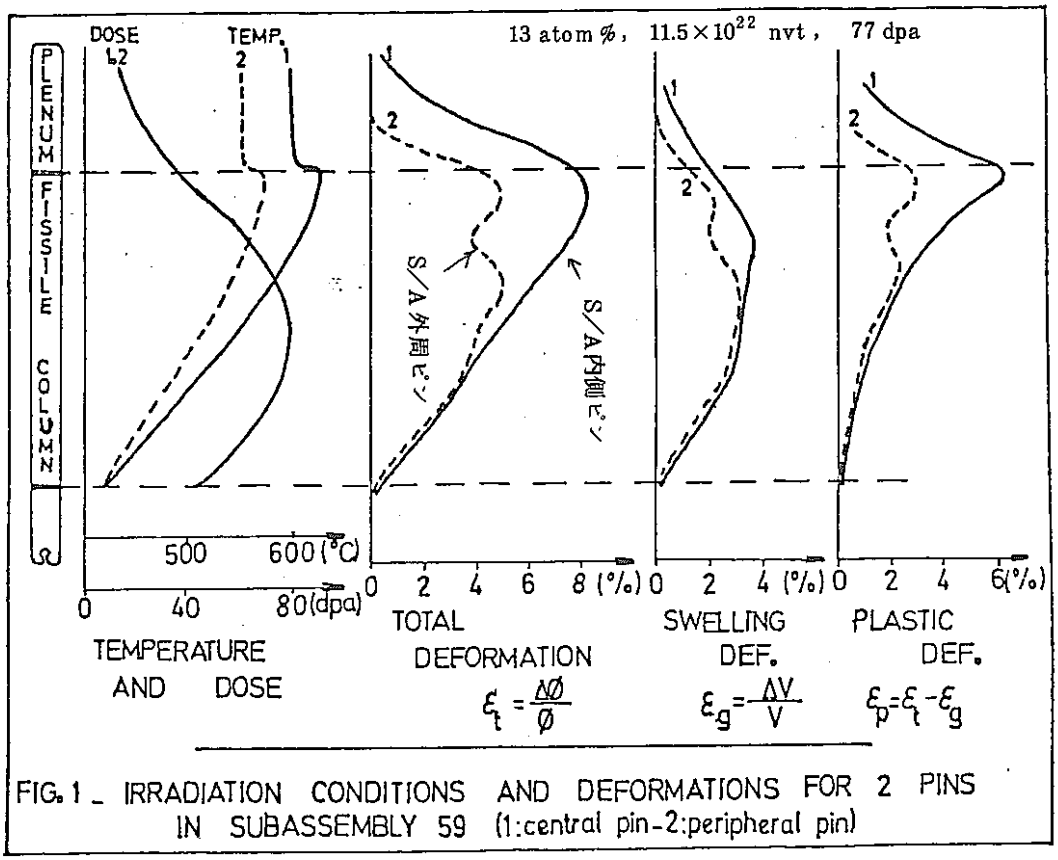

FIG. 1 _ IRRADIATION CONDITIONS AND DEFORMATIONS FOR 2 PINS IN SUBASSEMBLY 59 (1:central pin-2:peripheral pin)

日　本　②

PNC－2, PNC－4実験（Rapsodie）

約 1.2×10^{23} nvt で K材ピンは 2.4 ％

約 6.5×10^{22} nvt で S材ピンは 3.7 ％

◎各国の316系被覆管のピン照射の中でPNCの45年度試作K材は△D／D 最も小さいほう。米国のN lotはこれに近い。もんじゅ燃料密度が他の例に比べ低いことも関係していると思われる。

2　燃料ピンの使用限界，破損経験

米　国　⑧

○Run－to－Cladding Breach（RTCB）Testで16本のピン破損を経験したが，典型的な使用限界による破損は未だ生じてない（～14 at%まで）。

○破損原因の大半はS／A再組立時のピンの曲がり等によるlocal high temperature（破損部周辺の被覆管にferrite layer，σ相またはχ相の析出が見られる。破損部以外は通常組織）

○ loose bundleで経験したピン束振動による被覆管肉厚損耗からの破損はtight bundleの採用により解消された。

○破損はいずれも小さく，隣接ピンへの影響はなかった。

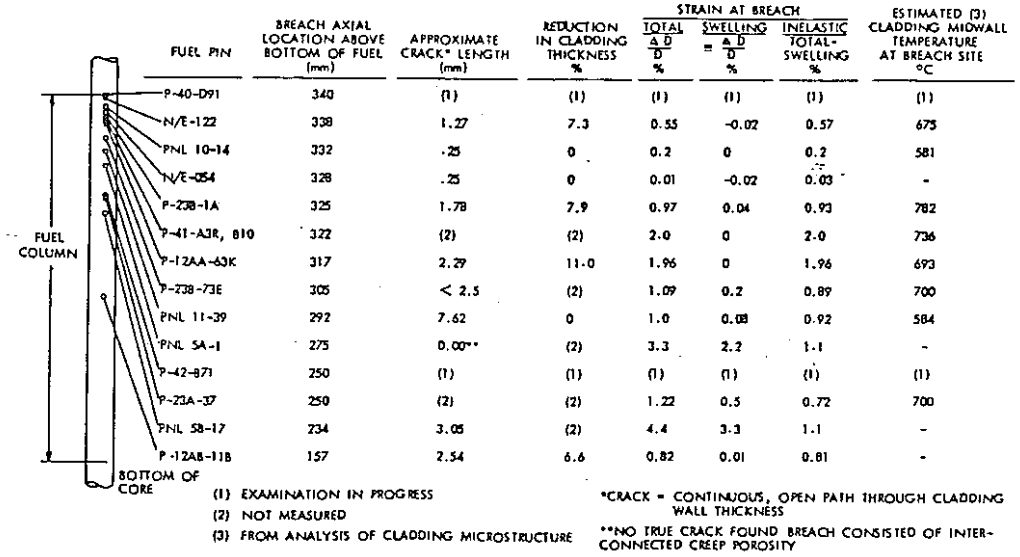

FUEL PIN	BREACH AXIAL LOCATION ABOVE BOTTOM OF FUEL (mm)	APPROXIMATE CRACK* LENGTH (mm)	REDUCTION IN CLADDING THICKNESS %	STRAIN AT BREACH TOTAL $\frac{\Delta D}{D}$ %	STRAIN AT BREACH SWELLING $= \frac{\Delta D}{D}$ %	STRAIN AT BREACH INELASTIC TOTAL－SWELLING %	ESTIMATED (3) CLADDING MIDWALL TEMPERATURE AT BREACH SITE °C
P-40-D91	340	(1)	(1)	(1)	(1)	(1)	(1)
N/E-122	338	1.27	7.3	0.55	-0.02	0.57	675
PNL 10-14	332	.25	0	0.2	0	0.2	581
N/E-054	328	.25	0	0.01	-0.02	0.03	-
P-238-1A	325	1.78	7.9	0.97	0.04	0.93	782
P-41-A3R, B10	322	(2)	(2)	2.0	0	2.0	736
P-12AA-63K	317	2.29	11.0	1.96	0	1.96	693
P-238-73E	305	< 2.5	(2)	1.09	0.2	0.89	700
PNL 11-39	292	7.62	0	1.0	0.08	0.92	584
PNL 5A-1	275	0.00**	(2)	3.3	2.2	1.1	-
P-42-871	250	(1)	(1)	(1)	(1)	(1)	(1)
P-23A-37	250	(2)	(2)	1.22	0.5	0.72	700
PNL 5B-17	234	3.05	(2)	4.4	3.3	1.1	-
P-12AB-11B	157	2.54	6.6	0.82	0.01	0.81	-

(1) EXAMINATION IN PROGRESS
(2) NOT MEASURED
(3) FROM ANALYSIS OF CLADDING MICROSTRUCTURE

*CRACK = CONTINUOUS, OPEN PATH THROUGH CLADDING WALL THICKNESS
**NO TRUE CRACK FOUND BREACH CONSISTED OF INTERCONNECTED CREEP POROSITY

Figure 1. Breach Location, Cladding Strain Measurements and Estimated Cladding Temperature at the Breach.

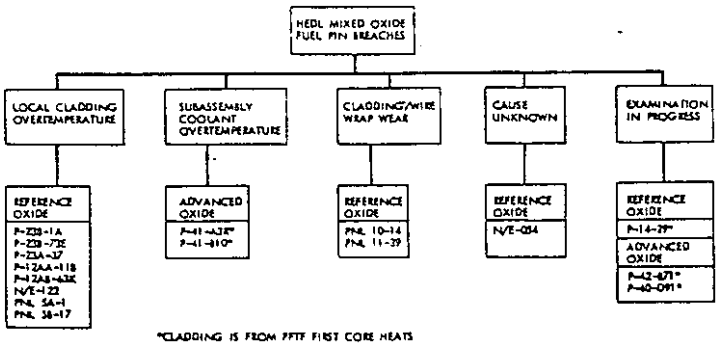

Figure 6. Classification of HEDL Mixed Oxide Fuel Pins Breached by Probable Cause.

英　国　⑤

M316ピンは 17.2 at%まで
FV548ピンは 18.5 at%まで
PE16ピンは 21.6 at%まで
} 破損しなかった。

○これより低いB.U.での破損のほとんどすべてがgas bulbleの附着（冷却材が下向流で流速が遅いDFR特有の現象）による。

TABLE II　STATISTICS FOR PINS IRRADIATED IN SUB-ASSEMBLY

Burn-up (% ha)	0-5	5-6	6-7	7-8	8-9	9-10	10-11	11-12	12-13	13-14	14-15
No. of pins	24_{4*}	3_0	10_0	18_{1*}	4_{3*}	5_0	2_0	12_{3*}	-	4_0	38_1

Subscript - No. failed pins.　　* Failures due to hot spots.

↖これも恐らく hot spot

hot spot ＝ gas bubble附着による局所過熱

○破損起こっても隣接ピンへの影響ない。

フランス　④，⑭

○ endurance limitによる破損は未だ1件も発生していない
（Fortissimo S/Aの最高到達B.U ≈ 160,000 MWD/T_{oxide}）

○初期破損（溶接欠陥による？）はRapsodie，Phenixの両方で経験，ガス・リークのみ。
Phenixでの破損本数は不明。（④ P. Coulon氏 口答説明）

日　本　②

○K材ピンは14 at.%で未破損（Rapsodie PNC－4）

○DFR 332/5，Rapsodie PNC−2（S材ピン）の破損はlocal overheatingによる。

○DFR 332/10（RTCB実験）の破損は高温＋高圧（プレナム体積小）による（？）
（～13 atom%）

3　破損ピンの継続照射

米国（Run Beyond Cladding Breach Test）　⑨

① 人工欠陥ピン照射

6～8 atom%まで照射したピンに人工欠陥（2～6㎝長さのスリット）を与えたピンを2.5～8時間照射（$PuO_2 - UO_2$）。

- DND（遅発中性子検出器）のシグナルは出力に対し指数函数的に増加（UO_2欠陥ピンの場合直線的に増加した）。
- クラックの拡大が生じたが，fuel lossは認められなかった。

② 炉内破損ピンの継続照射

○ピークB.U. 10.8 atom%の37本ピンS/AでFPガス．リークが検出され，その後5日間照射継続した後炉停止。

○6ヶ月間の冷却期間をおいて照射を再開。炉出力が50MWに到達したところでDNDシグナル急上昇。全出力到達後5日目にDNDシグナルがEBR－Ⅱで設定した許容値（800 cps）に到達したため炉停止。

○破損は最外周の1本のピンの燃料カラム下から約2/3のところに生じており（クラック長さ4㎝），隣りのピン表面の破損口に面した部分に変色が見られた。破損口からの燃料ロスは認められなかった。

◎以上の実験結果から

○安全上の問題を生ずる前にDNDで破損を十分検知できる。

○破損後のピン径増加（Na浸入後）は，それほど急速でなく，破損口からの燃料ロスも起こらない。

英　国　⑩

○炉内破損ピン，人工欠陥ピンを含め47本の欠陥ピン照射を実施（DFR）。

照射継続期間	60 ～ 320日
燃　焼　度	0～14.4 atom%
被　覆　管	M316, FV548, PE16

（結　果）

○低燃焼度ピン（＜5 atom%）の場合，被覆管温度500℃以下では150日くらいまで破損口拡大は起こらない。高温では破損口拡大あるが，M316では拡大小。

○高B.U.になると破損拡大はより顕著になる。

○破損後の△D/D増加はO/M比大きいほど大。

○燃料密度，形態（ペレット，vibro），線出力等の破損拡大への影響は少い。

◎一般的に高燃焼度ピンでも破損拡大はそれほど急速には起こらず，破損発生後少くとも60日くらいの照射継続は許容できる。

4 燃料の熱的挙動

米　国　㉒㉓

○ EBR－Ⅱにおける Power － to －Melt（Q_m）実験

（P－19, P－20 実験結果）　㉒

燃料密度＝90.4％TD，ピン外径 5.84㎜，被覆管内面温度 571℃のときに，

- fresh 燃料の Q_m はギャップ寸法に大きく依存し，gap ＜ 100μ では Q_m ～ 600 w/㎝，gap 大 → Q_m 小
- ピン内充填ガス（通常 He）に Xe（タグ．ガス）が混入すると Qm は低下する。

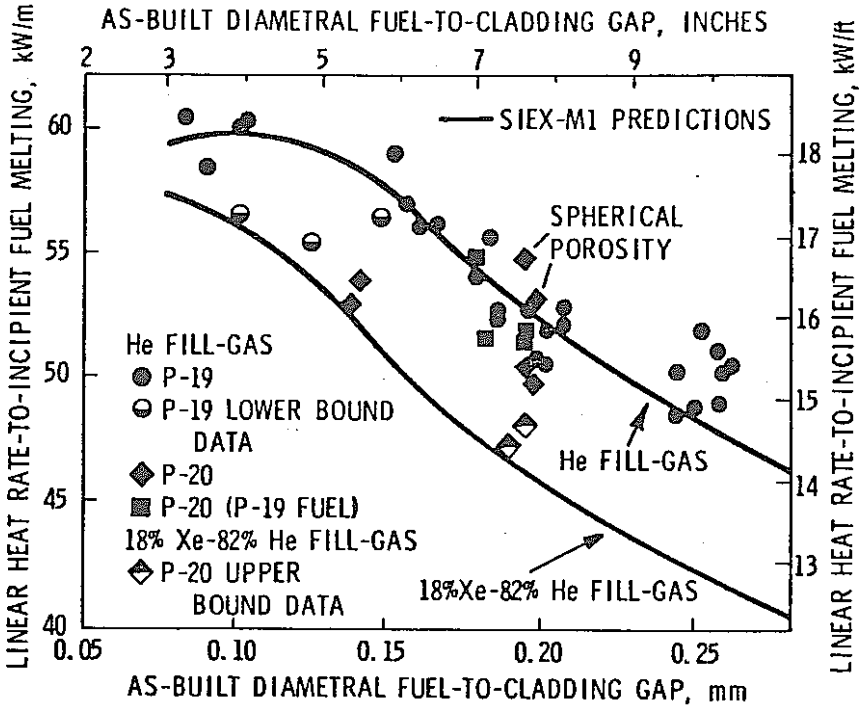

Figure 3. Normalized Power-to-Melt, Q'_m, Data for Fresh Fuel.

- 0.38 atom%まで前照射（precond-itioning）すると製造時ギャップの大きな燃料も Q_m が増加し，少なくとも 610 w/㎝以上になる。

gap closure
組織変化　} による

熱的特性改善のあらわれ。

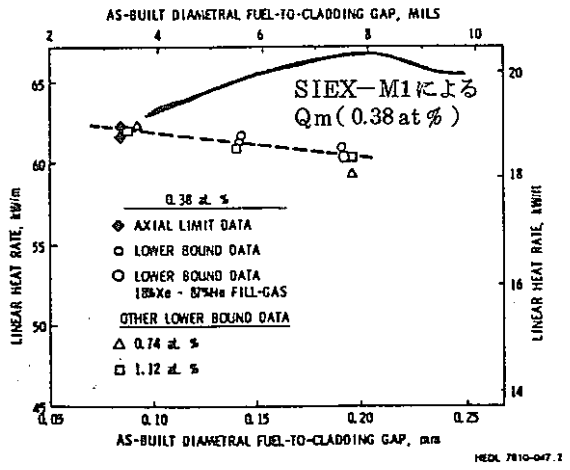

Normalize Q'_m or Peak Power Values for Fuel With Preconditioning.

（GE　F－20実験結果）　㉓

- Qm（Power－to－melt）に対するギャップの効果のほかに，燃焼度，及び燃料密度の影響を調べた。
- Qm（照射開始時約560w/cm）は約10日間の照射（0.3 atom%）でギャップが閉じ，組織変化の影響もあって620w/cmくらいまで大きくなるが，高燃焼度（6～9atom%）になると再び初期の値程度（～570w/cm）まで低下する。（主に燃料の熱伝導度低下による）

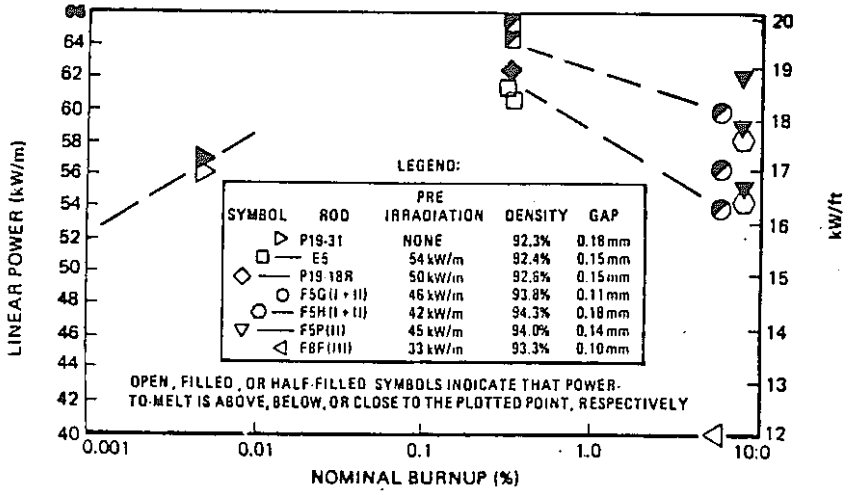

Figure 2. Effect of Irradiation on Power to Melt (0.11-0.18 mm Gap, 92.3-94.3% Density

- preconditioningした燃料のQmは製造時燃料密度が低いほうが大きくなる。（低密度燃料ほどpreconditioning時の組織変化が大きいため）。

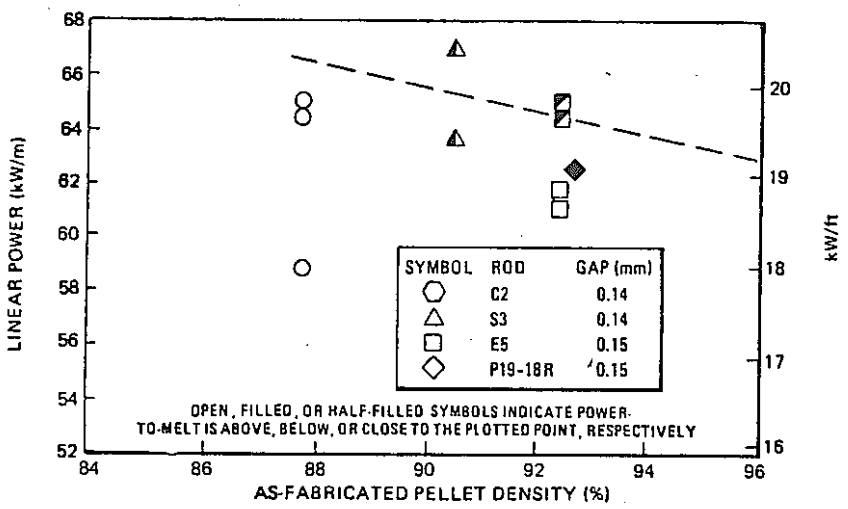

Figure 3. Effect of Fuel Density on Power to Melt of Low Burnup (0.3% - Phase I & II) Fuel

フランス　㉖

○燃料中心温度測定（ラプソディ炉）

・燃料中心にW／W－Re熱電対を入れて照射中の温度測定

・パラメータ：O／M比，ギャップ寸法

（O／M比の影響）

・燃料中心温度は，炉外測定から得た熱伝導度のO／M比依存性から予測されるほど大きくO／M比によって変ることはなかった。→ O／M比再分布がかなり短時間のうちに起こり低O／M比燃料でも外周領域は2.00に近くなってしまうため（？）

（初期ギャプ寸法の影響）

・小ギャプ（≦71μ）の燃料の場合full power到達後の温度は一定。

・大ギャップ（≦140μ）の燃料の場合，full power到達時に最高温度に達し，その後約10hrの間徐々に低下してその後一定になる。

↓

rapid gap closureによる。

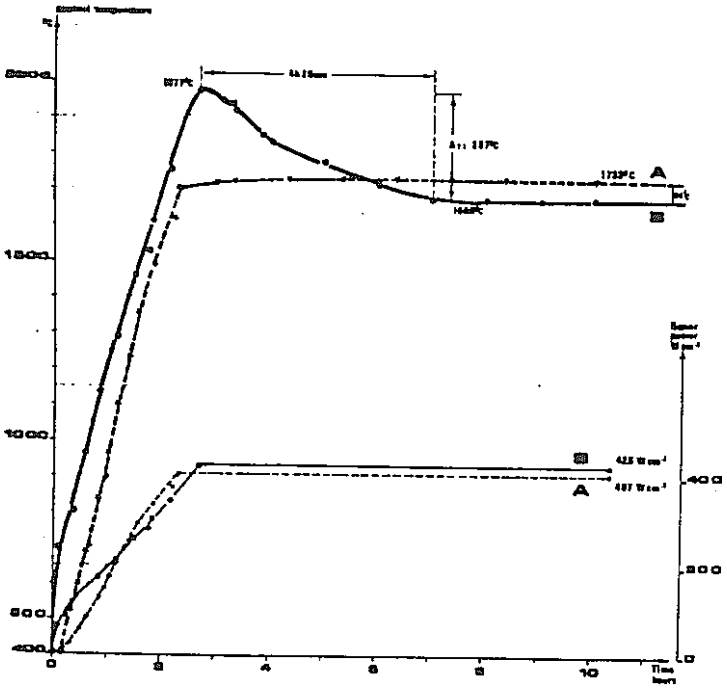

Fig. 7 - Measured central temperature as a function of time for A and B experiments.

O/M = 1.986

日　本　②

○GETR－T実験（溶融実験）から，Joyo型燃料Power－to－meltは611±60 w/cmと評価された。

5　ＦＰガス放出率

米　国　①

○ＦＰガス放出率に関する経験式：

- ＥＢＲ－Ⅱ照射燃料ピンのデータによる。
- ＦＰガス放出率（Ｆ）

$$F = F_r + F_u$$

F_r ＝ 組織変化領域からの放出率

F_u ＝ 組織不変領域からの放出率

$$F_r = 0.08 + 0.92\{1 - 0.86[1 - \exp(-B/5.9)]/B\} \quad (1)$$

and

$$F_u = 1 - 7.3\{1 - \exp[-(B - 3.5)/3.5]\}\{\exp(-0.001\ q_l)\}F'(B) \quad (2)$$

B = local burnup, MWd/kgM
ql = local linear heat rate, W/cm
F' = 1 for B > 50.0,
= exp [-0.3(B - 50.00] for B < 50.0.

- B.U. ＞80 MWD／Kg では放出率は１００％に近づく。
- 燃料中に保持されるＦＰガスの量が最大になるのはB.U. ５０MWD／Kgより小さ目のところ。

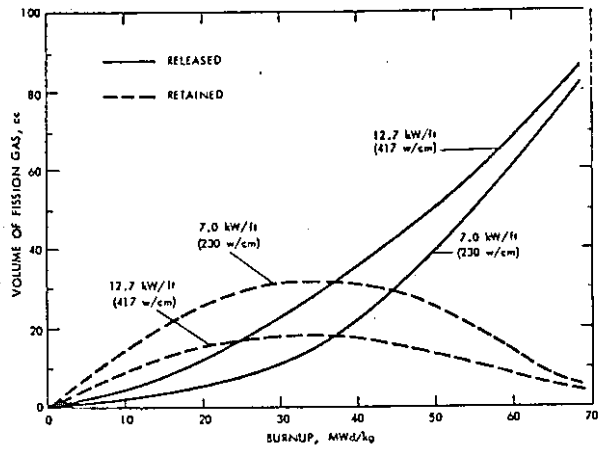

Figure 5. Calculated Released and Retained Fission Gas vs. Peak Burnup for Mixed Oxide Fuel Irradiated in E8R-II.

西　独　　③

○ＦＲ２実験で得られたＦＰガス放出率（Fig.1）

○Mol －8Ｃ実験におけるＦＰガス蓄積測定結果

（Fig.4）

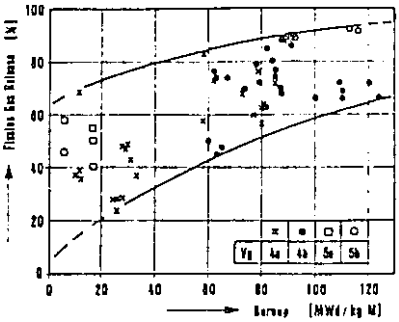

Fig. 1: Fission Gas Release of UO_2- PuO_2 Pins in FR 2 Capsule Tests

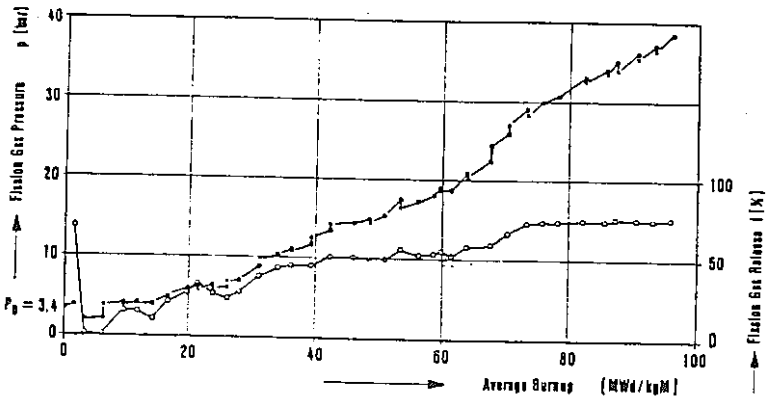

Fig. 4: Fission Gas Pressure Buildup and Release Rate Irradiation Mol-8C, Pin 8C-4

6 FCMI (Fuel-Cladding Mechanical Interaction)

米　国　　⑬，⑩，⑯

○WSA－3実験（密度，ギャップをパラメータとした燃料ピン照射）でmax△D／Dは燃料のスミア密度に依存することが明らかになった。→FCMIがあることを示している。（Fig.1）　－⑬

○燃料スミア密度を1％高くしても，直径ギャップを25μ増加させると密度増加の効果は打消され，燃料ピン径変化は同じになる。（Fig.2，Fig.3）　⑩

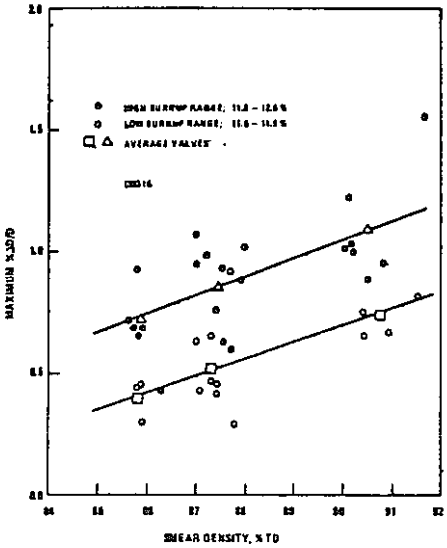

Fig. 1. WSA-3 Data Analysis

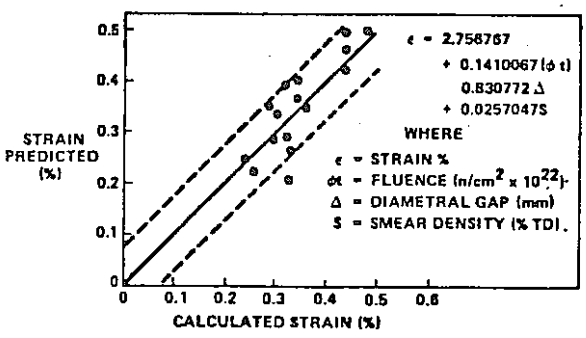

Fig. 2 REGRESSION ANALYSIS OF WSA-3 STRAIN DATA

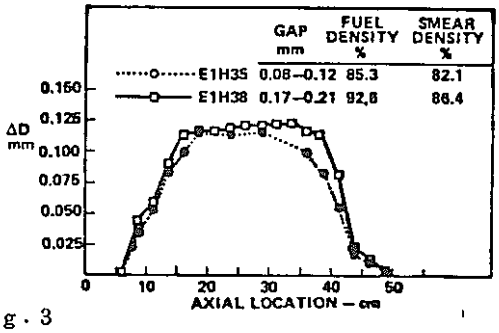

Fig. 3
PROFILOMETRY DATA COMPARISON FOR PINS E1H35 AND E1H38

○WSA－3の各ピンのプレナムガス圧測定結果と，使用したN lot被覆管に関する照射クリープ式をもとに，FPガス圧のみによるピン外径変化量を計算し，これらを実測値と比較したところ，後者のほうが明らかに大きく，FCMIによる歪みが発生していることが示された。（Fig.4）　⑯

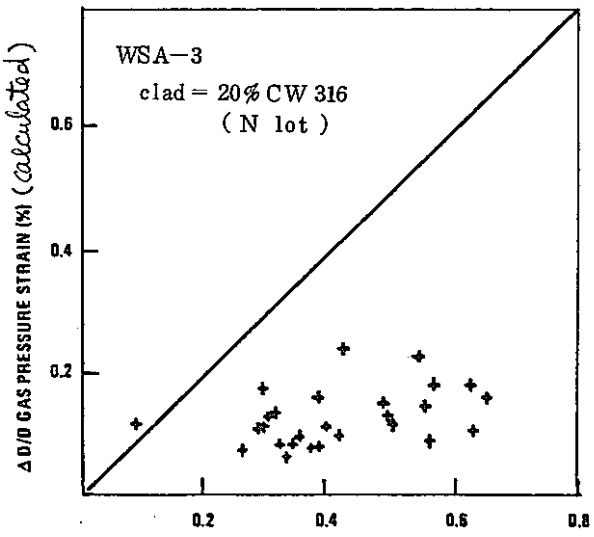

Fig. 4 ΔD/D MEASURED MECHANICAL STRAIN (%)

〔ＬＩＦＥ－３コードによる大型炉燃料のＦＣＭＩ解析の例〕　㊻

○炉心燃料ピンの場合　定常時のＦＣＭＩはＣＤＦ*にあまり寄与しない。しかし，定常状態でＦＣＭＩが生じている時にtransient overpowerが重なると，ＣＤＦをステップ状に増大させることになる。

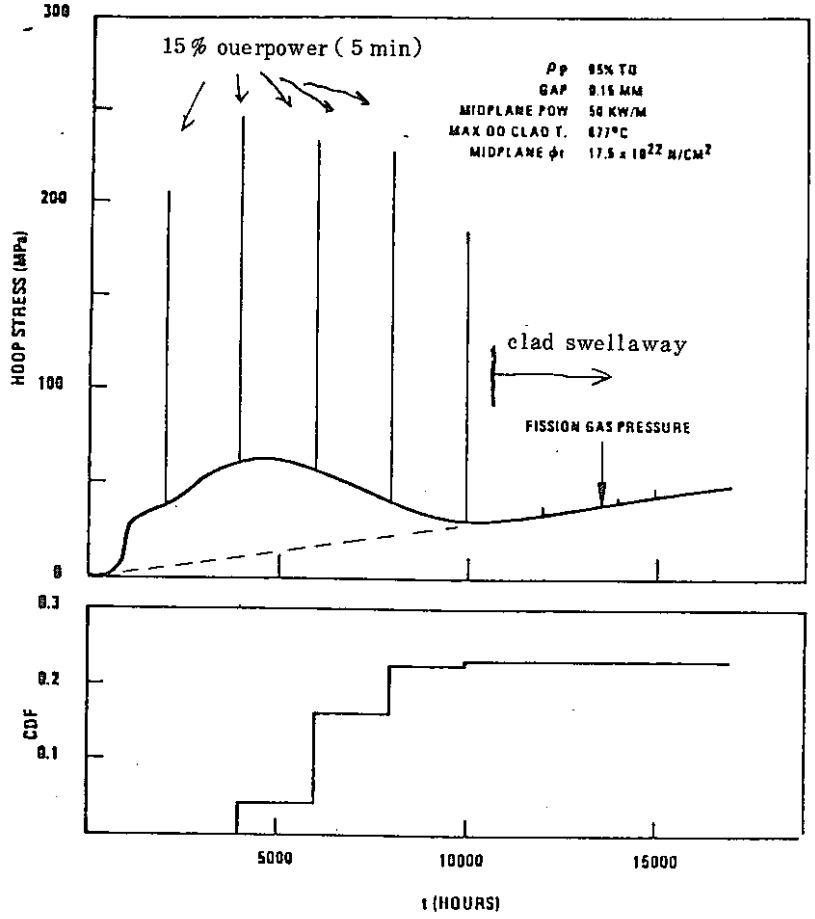

○ブランケット燃料の場合　定常時，過渡時ともにＦＣＭＩはＣＤＦ増大につながらない。ＥＯＬで被覆管温度が上昇してきたときのＦＰガス内圧がＣＤＦを増大させる。

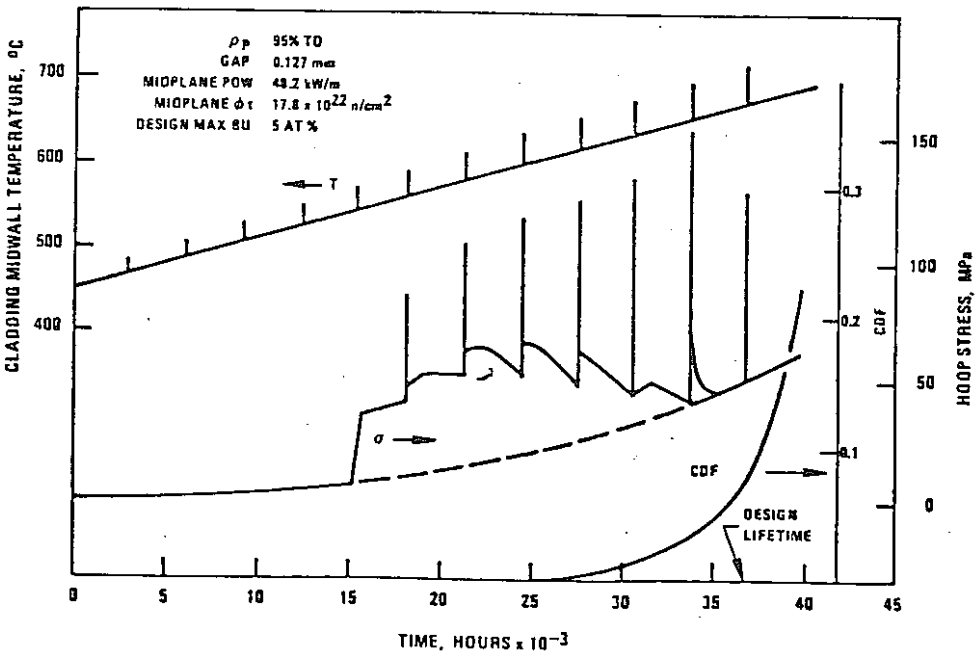

＊ＣＤＦ（Cumulutive Damage Fraction）：被覆管のクリープ寿命損傷和

日　本　　②

○被覆管の機械的歪みは燃焼度が4～5 atom% のところから顕著になる。この歪み立ち上りの時期はギャップが閉じ終る時期と一致しており，歪みがＦＣＭＩによって生ずることを示している。

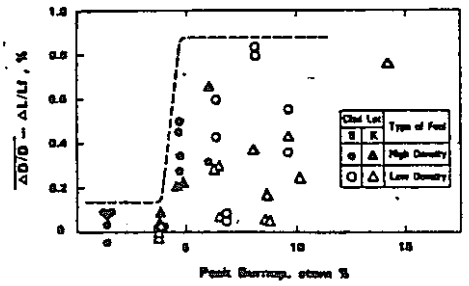

Fig. 5. Mean Inelastic Strain V.S. Burnup

○燃料スミア密度が低くなると被覆管の歪みも低減する。

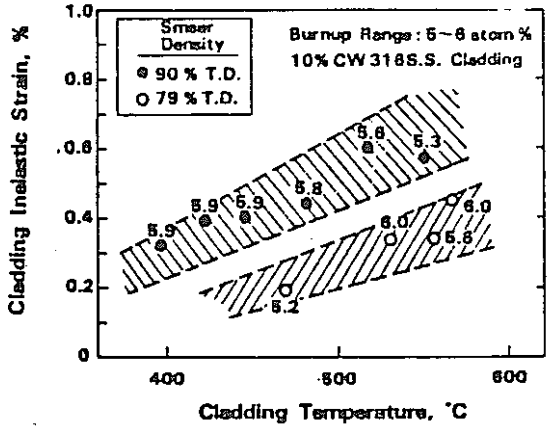

Fig. 7. Effect of Fuel smear Density on Cladding Inelastic Strain

フランス　　㉑，㊹

○ＰhenixではＦＣＭＩによるとみられるピンの径増加は全く認められない。

○Ｒapsodieの燃料ピンの径増加も，ＦＰガス圧によるもので，ＦＣＭＩの影響は全くないか，無視できる程度である。

○ギャップ寸法が極端に小さければＦＣＭＩ起こることもあるが，通常はＦＣＭＩは問題とならない。

（ラプソディ炉で30～40μギャップの燃料（O／M比 2.00, 1.97, 1.93)を照射したところ，O／M＝1.93の燃料ピンが約30日目に破損した例がある。）

○Phenixで full powerの2／3での運転が150日続いた後，full powerに出力を上げた時にも何のトラブルも生じなかった。

○通常ＦＣＭＩは全く問題とならないが，過渡現象が伴うと重要な問題となるだろう。（load－following operation等）。

7 FCCI (Fuel－Cladding Chemical Interaction;被覆管内面腐食)

米　国　㊳，㊼，㊴

○内面腐食深さについての経験式　㊳

・P－23シリーズの実験で観察されたＦＣＣＩの形態のB.U.別，O／M 比別分類

〔定義〕

・nominal depth：

横断面金相写真周方向８ヶ所のそれぞれの位置における最大腐食深さの平均値

・maximum depth：

ある断面における最大腐食深さ

O/M	BURNUP LOW (0-3 at.%)	BURNUP MODERATE (3-6 at.%)	BURNUP HIGH (6-10 at.%)
HIGH (1.98-1.99)	>675°C** INTERGRANULAR <675°C MATRIX <500°C NO FCCI 7 PINS *	>675°C EVOLVED MATRIX <675°C MATRIX <500°C NO FCCI 2 PINS	>500°C EVOLVED MATRIX <500°C NO FCCI 4 PINS
MODERATE (1.98-1.97) *	>550°C MATRIX <550°C NO FCCI 10 PINS	>550°C MATRIX <550°C NO FCCI 3 PINS	>650°C COMBINED >525°C MATRIX <525°C NO FCCI 4 PINS
LOW (1.94-1.93)	>700°C SHALLOW MATRIX <700°C NO FCCI 3 PINS	>625°C SHALLOW INTERGRANULAR <625°C NO FCCI 4 PINS	>600°C SHALLOW INTERGRANULAR AND MATRIX <600°C NO FCCI 4 PINS

* NUMBER OF FUEL PINS EXAMINED WITH INDICATED O/M's AND BURNUPS

** CLADDING INNER SURFACE TEMPERATURE

Figure 2. Characterization of Fuel-Cladding Chemical Interaction in 41 Fuel Pins from the HEDL P-23 Test Series

〔経験式〕

$$D = .4521\,(B + K)(O/M - 1.942)(T - 728) \quad \text{for } B > 0,\ O/M > 1.942,\ T > 728$$

(for conditions outside this range, D is zero)

where:

D = Depth of cladding interaction (microns)
B = Local fuel burnup (atom %)
K = Constant (A function of the confidence level for maximum depth of interaction)
O/M = Initial as-fabricated fuel oxygen-to-metal ratio
T = Local time averaged cladding inner surface temperature (°K)

・この経験式は“nominal depth”，“maxinum depth”の両方に適用可。

・K＝0とすれば，Dは nominal depthを表わす。

・maximum depthを表現する時には必要とする信頼限界値の大きさに応じて次のような値をKに代入すればよい。

K	Confidence Level
12.23	95%
9.45	90%
6.66	80%
5.04	70%
3.00	50%

（例）

K＝12.23とすると，上式の予測値は95％の信頼度で実測のmaximum depth より小さくなることはない。

○ CCCT（Cladding Component Chemical Transport）　㊼

- 高O／M比，Temp ＞ 600℃，B.U. ＞ 5 atom％で観察される被覆管内面の剝離現象
  → 通常の化学反応としては説明しきれない。
- 被覆管成分（Fe，Ni）が，ギャップにたまったTe，Cs（液相）に溶出し，温度が高い燃料側にdepositするというメカニズムによると考えられる。

Step 1 - formation of Fe, Cr and Ni tellurides (MTe_n) at the cladding inner surface (T_1);
Step 2 - dissolution of MTe_n compounds in the Cs-Te melt;
Step 3 - transport of dissolved MTe_n up the radial temperature gradient;
Step 4 - decomposition of MTe_n, and deposition of M, at some high temperature location in the fuel (T_2);
Step 5 - return of Te and Cs down the thermal gradient to the cladding inner surface;

or, expressed as a reversible reaction, $[M]_{clad} + n[Te]_{melt} \rightleftharpoons [MTe_n]_{melt}$

T_1(ca 650°C) → T_2 ($T_2 > T_1$).

- 被覆管内面腐食は通常の化学反応的ＦＣＣＩに上述のＣＣＣＴの効果が重なって現れる。

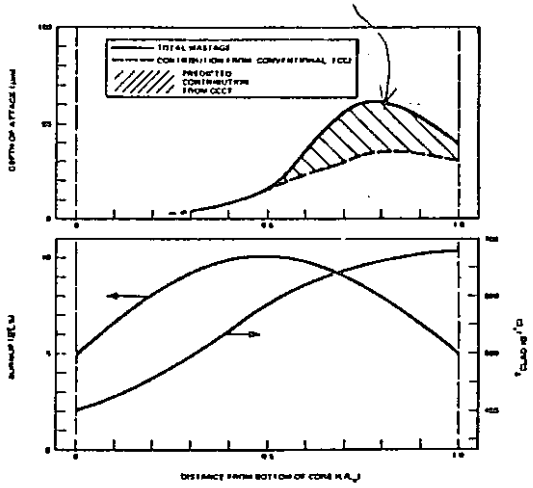

Figure 3. Prediction of Axial Distribution of FCCI-Induced Cladding Wastage in Long, Commercial-Type LMFBR Fuel Pin.

○内面腐食低減化対策（Buffer／Getter 材）　㊴

- Ｖ，Ｎｂのコーティング（ペレットの側面，または端面 － いずれでも効果は大差なし）は内面腐食を抑える効果顕著。
- 腐食低減化材としてはＶ＞Ｎｂ＞Ｔｉ＞Ｃｒの順で有望。Ｃｒはほとんど効果なし。
- Ｎｂ，Ｔｉ等の porous metal pellet を燃料カラム両端に酸素ゲッターとして入れたが，これは役立たなかった。
- Ｖ，Ｎｂ等は燃料ピンの軸方向にある程度均一に分散させておかないと効果がない。

英　国　　⑳

○通常のFCCIは500℃以上で観察される。データは600℃近辺にピークを示している（Fig. 1）。この温度領域ではFCCIに起因する破損はない。

○FCCIの深さは線出力に依存（線出力大 → attack depth大）。

○B.U.依存性はあまり大きくはない。低B.U.でもかなり深いattackが起こることもある。

○穴あきペレットよりもVIPAC燃料のほうがFCCI大きい傾向認められる。

○Mk－Ⅶa実験のVIPAC燃料ピンは450～500℃の温度領域（通常FCCI起こらない）で被覆管の粒界割れを起こして破損。crackの端にTe，Cs，Mo等が検出された。（SCCに似た割れ）。

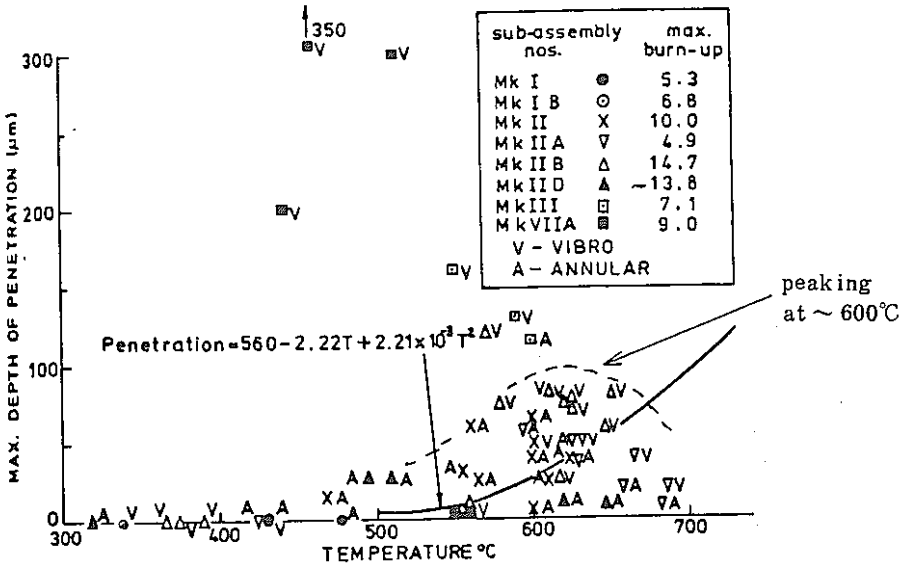

Fig.1. Relation of internal corrosion to clad temperature in stainless steel clad fuel pins.

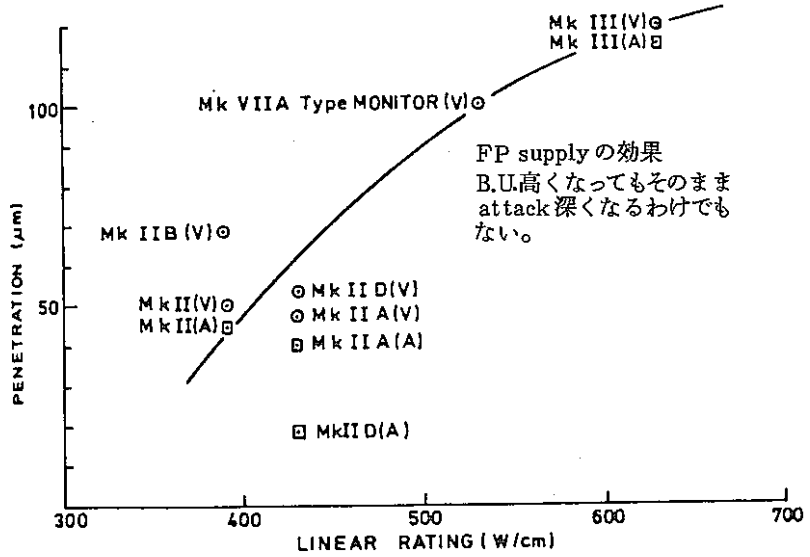

Fig. 2. Variation in clad corrosion with linear rating

ドイツ　　⑩

○内面腐食深さについての経験式

BR－2，Rapsodie，DFRで行なったSNR型燃料の照射実験データによる実験式。

$$C = 96.970\left[1-3.013\times10^{5}(2-O/M)^{4}\right]\exp\left(-\frac{76\cdot920}{T-769}\right)$$

which is valid for $1.96 \leq O/M \leq 2.00$ and for $769 \leq T \leq 923$ K only.

where C is the depth of the maximum total attack (μm),

T is the inner cladding temperature (K),

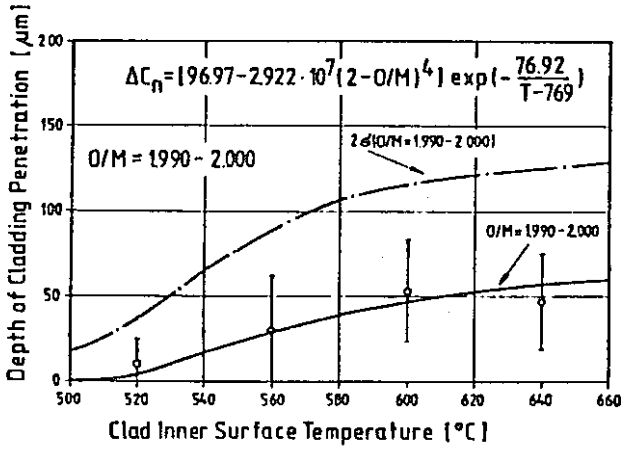

Figure 2: Depth of Cladding Attack as Funktion of Temperature for initial O/M-Ratio 1.990-2.000

日　本　　②

○一点のデータを除けば大体80μ以下。

○B.U.と必ずしも比例しない。

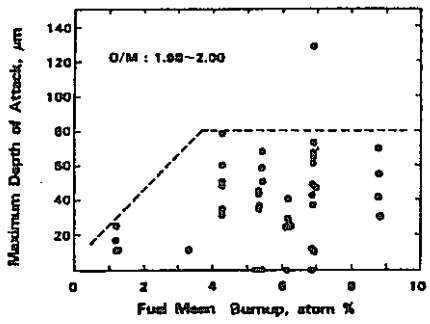

Maximum Depth of Cladding Attack V.S. Burnup

フランス　　⑭

○FCCIによるclad肉厚減は100000MWD／Tまで行っても100μを超えない。

8　Cs の 軸 方 向 移 行

米　国

（Cs移行の影響）

○Csは高B.U. では軸方向に移行しインシュレータ部に蓄積ピークを作る。こうしたCsの局所ピークの部分にしばしば被覆管△D／Dのローカル・ピークが生ずる（下図）。Cs移行はO／Mが低い燃料ほど顕著。

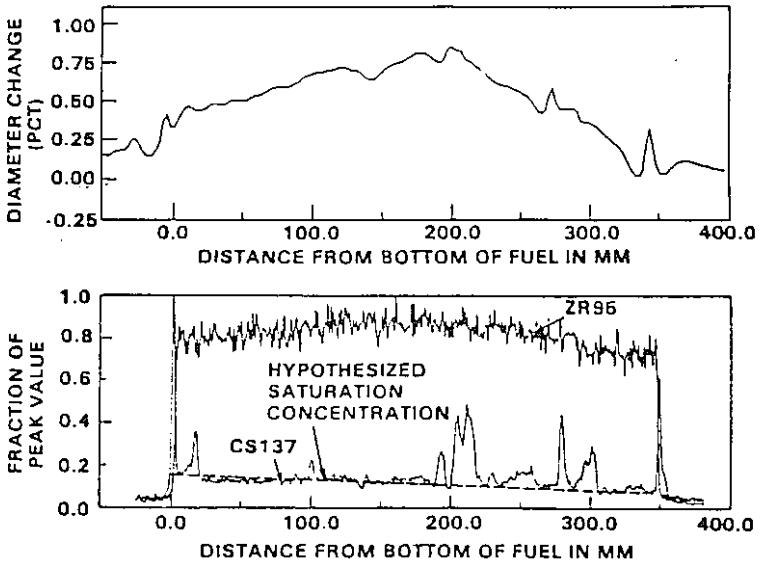

Figure 1. Profilometry and Gamma Scan Data from PNL-8-24.

（Cs蓄積，移行の実験式化）

燃料ピン内へのCsの蓄積には，ある飽和濃度（温度及びO／M比に依存）が存在し，これを超えてCsが蓄積すると，余剰分が軸方向移行を起こし，ローカル・ピークを生ずるという仮定に立ってEBR－Ⅱ照射ピンデータ（γスキャン結果）から次の実験式を作成。

〔データ範囲〕　EBR－Ⅱ照射ピン：33本

B.U.の範囲：2～9 atom%

〔結　果〕

①燃焼に伴うCs蓄積（生成）量：

$$Y_1 = \frac{0.1314 \times B \times W}{2\pi R} \qquad (1)$$

where:

Y_1 = The cesium concentration on the cladding inner surface (without axial migration) (g/mm²)
B = Local burnup (MWd/kg)
W = Linear fuel weight (total heavy metal divided by fuel column length) (kg/mm)
R = Cladding inner radius (mm)

② 飽和Cs濃度：

$$Y_2 = -1.2473 \times 10^{-3} + 7.3666 \times 10^{-4} (O/M) - 2.620 \times 10^{-7}(T) \quad (2)$$

where:

Y_2 = Cesium saturation concentration (g/mm^2)
O/M = Fuel oxygen-to-metal ratio
T = Cladding inner surface temperature (°C)

③ 余剰Cs量（軸方向に移行しローカルピークを作る）：

$$Cy = (Y_1 - Y_2)\, 2\pi RL \quad (3)$$

where:

Cy = grams of excess cesium (or, if negative, capacity to absorb excess cesium) in a segment of length L (mm)

④ 飽和Cs濃度の(1)式による予測と実測値との比較の例

（P－14－52：～80,000MWD／MTM）

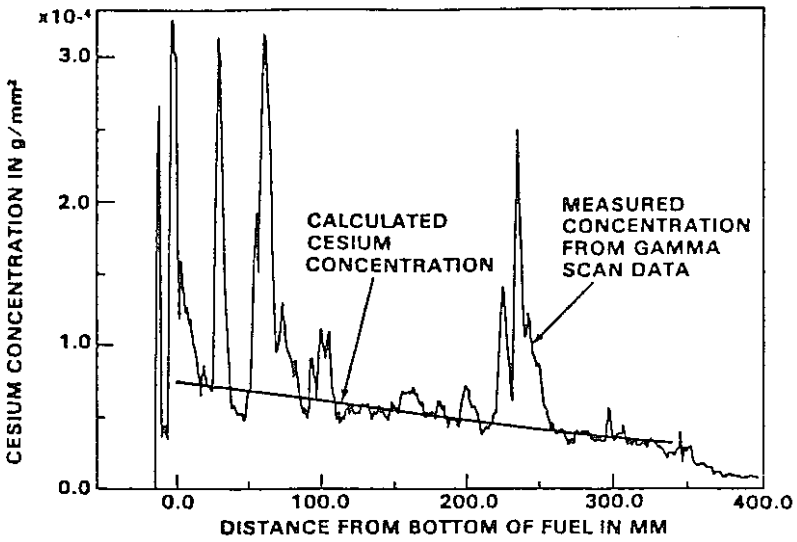

Comparison of Calculated and Measured Cesium Concentrations in P-14-52.

西　独　③

○ Rapsodie I 実験（ピークB.U. 95,000 MWD／T）の結果

- ピン上端側へのCs蓄積……

  O／Mに強く依存。

- ピン下端側へのCs蓄積……

  O／Mにあまり依存せず。

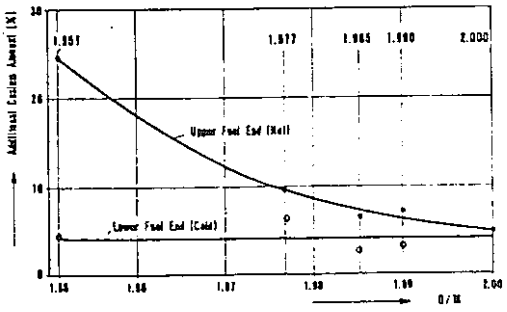

Fig. 6: Cesium Migration in Experiment Rapsodie I - Averaged Results of 33 Pins with Different Stoichiometry

日　本　　㉞

○Cs ピークがインシュレータ領域に生じていることを確認。

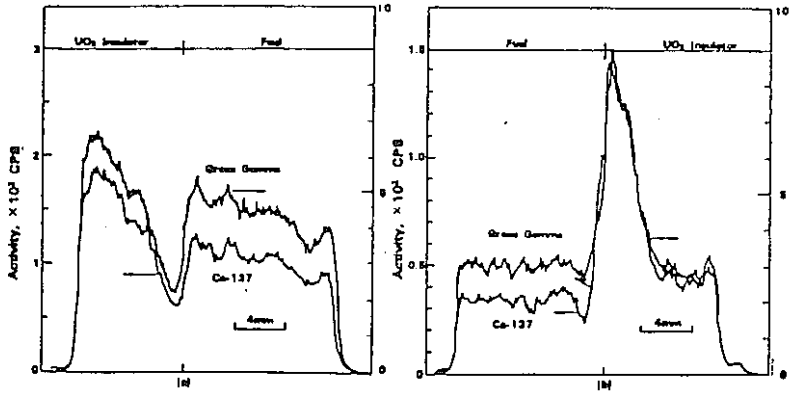

Fis. 2. Cesium Accumulation at Fuel/UO_2 Insulator Interface (a) Bottom Insulator Interface, (b) Top Insulator Interface Pin No. 1, DFR 332/7, Burnup 9.6 at.%, Power 420 W/cm

9　集合体としての高燃焼度照射実績

米　国　　①

○ PNL－13（FFTF第一炉心用被覆管使用，tight bundle）でpeak B.U.＝16.6 atom%（11.3 × 10^{22} nvt）。（モントレー会議原稿作成時点）

54／3／12～14 PNC／DOE燃材スペシャリスト・ミーティング（at HEDL）時の到達B.U.≒18 atom%。R.D.Leggett氏によればこの段階でS/Aを解体しようとしたところ，相当強いピン束－ラッパー管相互作用が生じており，通常の方法でピン束を引抜くことができなかったために，ラッパー管を縦割りにしたとのことであった。ピンはふくれのために隙間を奪い合うように絡み合っていたがピン破損はなかった。

英　国　　⑤

○Mk ⅡB S／Aで14.7 atom%（～1.4 × 10^{23} nvt）達成。

S／A内ではピン1本が破損したが，恐らくbubble附着が原因。

ドイツ　　③

○ Rapsodie Ⅱ S／A（ピン径7.6㎜）で約12 atom%達成（破損なし）

フランス　　④，⑪，⑭

○ Rapsodie－Fortissimoのドライバ－S／A

現在の標準B.U. ＝ 11 atom%（9 × 10^{22} nvt，60 dpa）

最大到達燃焼度 ≒ 160,000 MWD／T（oxide）（～19 atom%）

○ Phenix S／A

・最高到達B.U.＝72.000 MWD／T（oxide）

Phenix S／Aの最高B.U.はスウェリング／クリープによるラッパー管の変形（ふくれ，曲がり）によって制限される。

10 ピン束振動及びピン束／ラッパー管相互作用 (bundle-duct interaction)

米　国　　⑥1，⑥3

〔炉内実験〕

○ゆるい構造のS／A（porosity／ring＝5～6 mils／ring）ではピン束振動により被覆管と隣接ピンのワイヤーとがこすれ合い，被覆管肉厚損耗が起こり，一部ピン破損を生じた。
（PNL-9, 10, 11, NUMEC-E, F）

○きつい構造のS／A（porosity／ring ≒ 3 mils／ring）にしたところ上述のような問題は完全に解決された。（P-13, 14, 14A）
（P-13では18 atom%で相当厳しいbundle-duct interactionが生じたにもかかわらずピン破損はなかった。）

〔炉外実験〕

○FFTF／CRBRサイズのピン束（217本ピン）の6方向からの圧縮テストを行ない。bundle-duct interactionとpin-to-duct spacing及びpin-to-pin spacingの変化を調べた。

○きつい構造のS／Aではbundleーductinteractionがはじまるとfuelpindispersionが起こり，pin-to-duct spacing及びpin-to-pin spacingが徐々に減少。

○pin dispersionは個々のピンのflexible bending及びピン束全体のhelical bending（らせん状の曲がり）による。

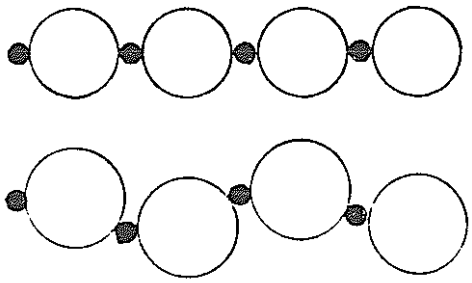

正規のピン配列

dispersionの例

〔bundle-duct interactionに対する設計基準〕

○FFTF／CRBRバンドルのpin-to-pin spacingの熱流力特性上の許容下限値は0.015インチ。
（冷却材流速が落ち，被覆管温度が局所的に上昇しないための最小spacing）

○CRBRのS／A設計ではbundle-duct interactionを「ワイヤ1本分」以下（＜1.5㎜*）に制限

＊　実際のワイヤー径＝0.056インチ（≒1.4㎜）

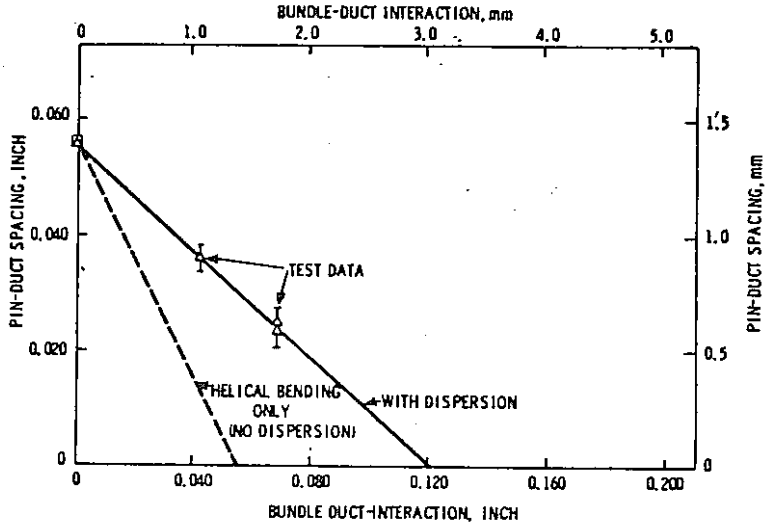

FIGURE 10. VARIATION OF BUNDLE-DUCT MINIMUM CLEARANCE WITH BUNDLE-DUCT INTERACTION.

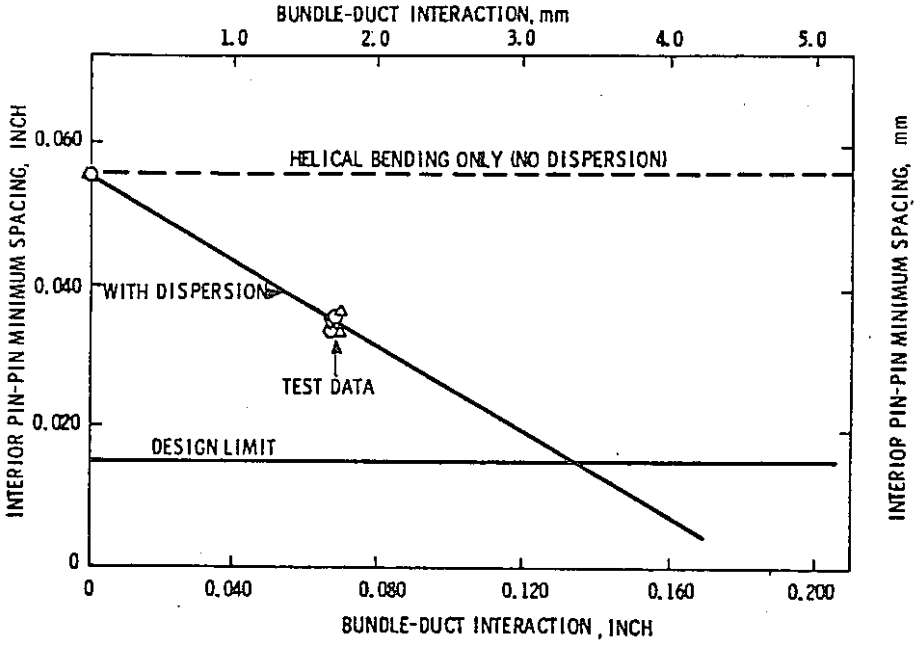

FIGURE 11. VARIATION IN PIN-PIN MINIMUM CLEARANCE WITH BUNDLE-DUCT INTERACTION.

フランス　　④，⑪，⑭

○ Rapsodie Fortissimo ドライバー燃料S／A*

B.U. ＝ 13 atom %，フルエンス＝ 1.15×10^{23} nvt で

max△D／Dの平均値≅ 6 %　　⑪

（*HEDL TME 75－48（ページV.C － 45）によるとFortissimo S／Aの porosity／ringのノミナル値は約4 mils／ring）

○ピン径がかなり増大してもcoolant flow rateへの影響は小さい。 ⑭
（max△D/Dが5％くらいまでは影響は小さい－④ P. Coulon氏口答説明）

○pin－to－pin contactはこれまで一度も経験してない。 ⑭

高フルエンスでのS/Aの変形

米　国　⑬

○FFTFでは燃料交換機の性能上からS/Aの曲がりの最大許容値を23㎜以下としている。

フランス　⑫，⑭

○PhenixにおけるS/A照射限界

- inner coreではneutron dose＜85 dpa
（S/Aの伸びとラッパ一管のふくれを許容値以下に抑えるため）
- outer coreでは照射日数＜400EFPD（～75 dpa）
（S/A曲がりを25㎜以下に制限するため）
- inner coreでのneutron doseの制限値は，燃焼度の低いS/Aで取り囲まれている時にはもう少しゆるめることもできる。

11　燃料ピン挙動のモデリング

米　国　　㊻，㊺，㊻，㊽

○LIFEコード開発の現状

LIFE－4（基本構造，解法はLIFE－3のまま，モデルの追加，改良が主）

LIFE－transient（LIFE－3またはLIFE－4に transient heat transfer routine を追加しただけ）

LIFE－3C（LIFE－3の炭・窒化物燃料解析用 version）

〔LIFE－4 追加／改良モデル〕

・O／M比再分布→Aitken／Evensのデータに基づくモデル

今のところ燃料熱伝導度にのみ反映

燃料クリープ速度に反映させるためのモデル修正進行中

・Pu再分布　→　Meyerのモデルによる。

径方向出力分布に反映

・燃料の融点

solidus temp. ……Pu／U比，O／M比，燃焼度に依存

liquidus temp. ……Pu／U比のみに依存。

melt boundaryは今のところ暫定的にSolidus temp.で決めている。

・燃料熱伝導度　→　燃焼に伴う変化をモデル化

① pore，bubble中のgasの効果を入れた（Marinoのモデルの修正）

pore中……プレナム・ガス組成と同じ
bubble中……ＦＰガス
} を仮定

② Solid ＦＰの効果

・初めＦＰ濃度増加とともに減少，やがて効果飽和。

・MgO－NiO系のデータを利用，最終的にはキャリブレーションの段階で調整

〔コード・キャリブレーション〕

LIFE－Ⅲ　・熱挙動計算／応力・歪計算のキャリブレーション完了

LIFE－4　・P－19，P－20（低燃焼度），F－20（高燃焼度）のデータにより熱計算部分のキャリブレーション進行中。

・応力・歪計算部分のキャリブレーションは未だ行なってない。

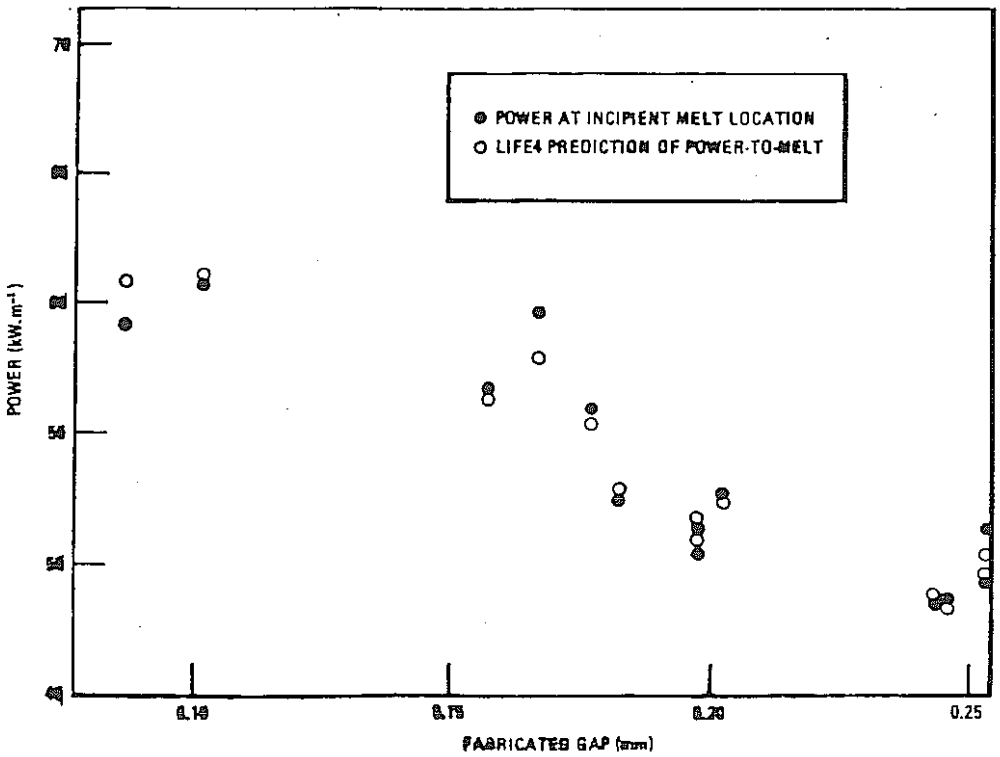

FIGURE 3. LIFE4 ANALYSIS OF P19 INCIPIENT MELT DATA

（P－19実験とLIFE－4による予測計算結果との比較）

〔LIFE－4によるFBRピンの熱挙動予測の例〕

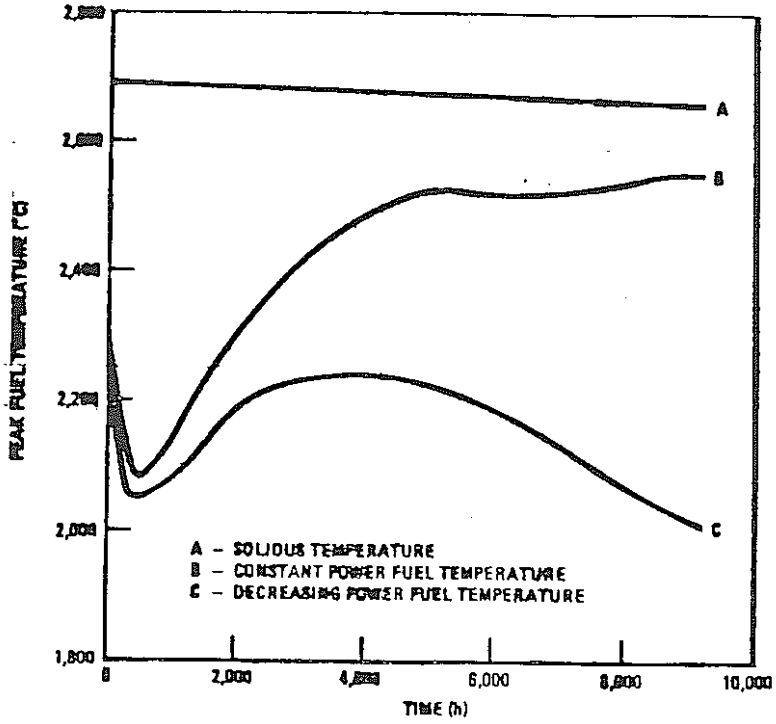

FIGURE 5. WHOLE-LIFE FUEL TEMPERATURE HISTORY

・計算条件：

BOLピーク線出力＝433 w/cm

ピークB.U.＝8 atom%

ピークフルエンス＝1.3×10^{22} nvt

・結果

初めの200 hrの間に組織変化とgap closureにより燃料中心温度は約400℃低下する。

その後燃焼に伴う燃料熱伝導度の低下やギャップコンダクタンス低下により再び温度は上昇する（ピン出力の低下を考慮に入れれば後半再び温度下降）。

gap reopeningがもし起これば末期の燃料計度はこの計算例により高くなる可能性ある。

西独／ベルギー　　㊼

○ IAMBUS（ Interatom社が1972～1975年の間に開発 ）

- 燃料と被覆管の間の摩擦力を考慮して径方向／軸方向の応力バランスを解く。
- ペレットの radial relotation の効果を考慮に入れた結果，炉停止後再び出力を上げた時に被覆管に応力のピークが生ずる（但し σ_y よりは大きくならない）。

○ COMETHE Ⅲ－J（ Belgonucleaire が1967年から開発 ）

- 経験式を多くして繰返し計算を少なくしており，EPRI が行なった LWP燃料挙動予測計算コンテストでは計算時間最小であった。
- ペレットの radial relocation はモデルとして入っていない。燃料の（ gaseous f.p. による）スウェリングのモデルに hydraustatic pressure の効果を生かすことによって照射初期の gap closure を表現している。

（COMETHE，IAMBUSに含まれるモデルの比較）

Topic	Feature	Status for FBR Fuel Rods	
		COMETHE III-J	IAMBUS
Fuel Analysis	Plasticity	T/IN	T
	Thermal creep	TI	T
	Irradiation creep	NT	T
	In-pile sintering	T	T
	Spontaneous radial relocation of fuel pieces	NT	T/IN
	Solid fission product swelling	T	T
	Fission gas bubble swelling	T	TI
	Hot pressing	T	NT
	Cracking and crack healing	T	T
	Pore migration and densification	T	T
	Equiaxed grain growth	T	NT
	Pu and O_2 migration	T	T
	Fission product transport	NT	NT
	Fission gas release to plenum	T	T
	Indigenous gas release	NT/IN	NT/IN
Cladding Analysis	Plasticity	NT	T
	Thermal creep	T	T
	Irradiation creep	T	T
	Void swelling	T	T
	Failure criterion	T	T
	Corrosion	IN/T	T
General Analysis	Gap conductance	T	T
	Radial mechanical interaction, FCMI	T	T
	Axial interaction, friction forces	NT	T
	Hot internal pressure	T	T
	Channel hydraulic analysis	T	IN

Footnote
T : Treated explicitely by mechanistic or empirical models
TI : Treated indirectly (with or without input support)
IN : Effect in input directly
NT : Not treated

英　国　　㊽

○ FRUMP コード

・各部分のモデルはできるだけ理論に忠実な形をとっている。

・フィッティングは，コード全体をマクロに行なうのではなく，むしろ，各部分モデル毎に，それぞれの未知数を，それを決めるのにふさわしい実験データをもとに半経験的に決めるという方式をとっている。

・解法としてはCrank－Nicholsonの方法に従っており，非線型の問題を線型化近似することにより（クラック・パターンを決める部を除いては）繰返し計算の必要性をなくしている。

〔モデルの特徴〕

・組織変化の詳細な取扱い

・vibrofuel の特殊な取扱い

・定常時のＦＰガス挙動モデル

組織不変領域及び等軸晶領域については粒内ガスバルブの粒界への拡散による移動を計算。粒界に到達したガスの一部は放出され，一部は燃料スウェリングに寄与（→初期の gap closure に影響大）

・過渡時のＦＰガス挙動モデル

Wood／Hayensのモデルの簡略化

ＦＲＵＭＰによるＦＰガス保持率分布予測と実験結果との比較　→

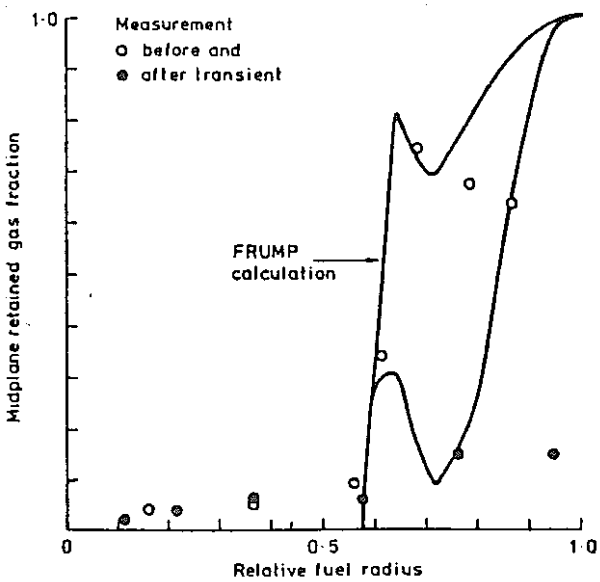

Fig.2. Radial Gas Distribution before and after the TREAT H3 Test

日　本　　㊾，㊾

○MIPEC－RZ（PNCからの委託で日立が開発）　　㊾

- PCMI解析に主眼を置いたコード
- gap closureの要因として照射開始時のペレットの径方向リロケーションを考慮してモデル化 － Jump Relocation Model

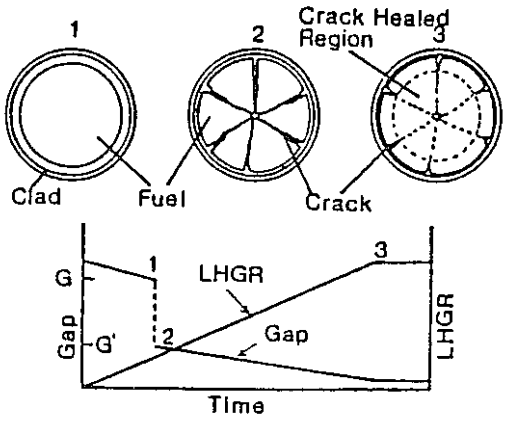

Figure 1. Jump Relocation Model for Cracked Fuel

- クラックの入った燃料の取扱い：

  LIFE－Ⅱと同様にクラック数の増加に伴いYong率を小さくしているが，Poisson比の取扱いについて二通りのオプションを持っている。

○FIBER－H（MAPI開発）　　㊾

- FIBER（CYGROをベースとしたコード）のHybrid版。
- 組織変化計算はPIEデータに基づく経験式を用いることにより簡略化
- 短時間塑性歪み量計算 → FIBER－Ⅱ（FEMコード）によるパラメトリックサーベイの結果を実験式的に利用。

12　新型および代替燃料（米国）

(1) 照　射　計　画　　㊾

米国では，NASAP（Nonproliferation Alternate System Assessments Program）あるいは，INFCE（International Nuclear Fuel Cycle Evaluation）と関連付けて，ウランとプルトニウムの酸化物燃料以外の様々な燃料についての照射試験及びその評価が，1977年～1979年に渡って計画され，実行されている。その燃料としては，

トリウムベース燃料……$(Pu, Th)O_2$，$(Pu, Th)C$，$(^{233}U, ^{238}U)O_2$，$(^{233}U, ^{238}U)C$

金属燃料……$U_{0.15} \cdot Pu_{0.10} \cdot Zr \cdot Th_{0.15} \cdot Pu_{0.10} \cdot Zr$

炭化物燃料……Na封入，He封入

などが挙げられている。

(2) 炭 化 物 燃 料

○Naボンドピン　　㊿

EBR－Ⅱで計113本の燃料ピンが照射された。照射がそれ程進んでいない段階（3 atom%）でPCMIによると思われる破損が生じた。しかし，ピン内にシュラウドチュウブを入れるなり，被覆管の材質を強化し，またその肉厚を多くすれば，そのような破損は防げる。

（照射後試験結果）

- 燃料スウェリング……炭化物の組成の中で，M_2C_3の多いものの方がスウェリングは小さい。

  M_2C_3のほとんどない場合：3.0 vol%／at.%

  M_2C_3の比較的多い場合　：2.4 vol%／at.%

- シュラウドチューブの挙動……燃料が割れて動くのを防いでいることは明らか。
- ピン変形……内部（PCMI）と外部（スペーサーと被覆管）の両方の機械的相互作用が発生している。

  シュラウドなしのピンでは照射初期から変形が生じる（Fig.1）。スペーサー付きのピンでは，ワイヤーによる変形が観察され，破損した1本のピンの破損箇所は，集合体のダクトにワイヤが接触している地点で発生した。
- 被覆管の浸炭……被覆管の炭化の度合は硬度測定で判定。

  M_2C_3の含まれる燃料では，0.11㎜の深さまで硬くなっているが，MCだけの燃料では硬さ変化はほとんど見られない。400℃～600℃の温度範囲では，炭化の度合は，被覆管の材質に無関係。

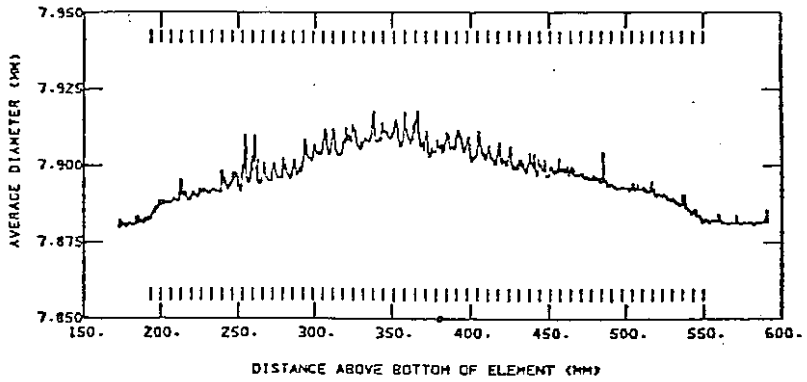

Fig. 1 Average cladding diameter of element K4-1. Vertical ticks at the top and bottom of the plot represent axial locations of pellet interfaces.

・ＦＰガス放出……放出率は３～１４％。

○Ｈｅボンドピン　　㉑

ＥＢＲ－Ⅱで合計１７１本のＨｅ封入炭化物燃料ピンが照射され，既に一部の燃料ピンの照射後試験が完了している。破損はたった１本に発生しただけであった。Ｈｅボンド炭化物燃料ピンの場合，ＰＣＭＩによる被覆管の歪みが大きいが，それと，炭化物組成（M_2C_3の割）との相関は明らかで，燃料密度やダイヤメトラルギャップ等のパラメーターとの関連も，今後の照射後試験結果から詳細に明らかとなるだろう。

（照射後試験結果）

・金相写真……各金相断面写真からは特に異常は見られない。

燃料組成（M_2C_3の割合）の大きく異なる場合でも，金相写真やα－オートラジオグラフィーに差はない。燃料密度８１％でダイアメトラルギャップが０.１３㎜のピンと各々８８％，０.２５㎜のピンを比べると，前者の方のスミア密度が３％程小さいだけであるのに，空孔の多い領域（Ｐｏｒｏｕｓ Ｚｏｎｅ）内側直径が４６％と後者（６３～６７％）と比べ大きく異なる。

・ＦＰガス放出……以前行なわれた試験ではＨｅボンド炭化物燃料のＦＰガス放出率はスミアー密度と逆比例した。Ｋ６ＡとＫ６Ｂのシリーズのスミア密度８１，７８，７５％のピンのＦＰガス放出率は，各々８％，１３％，１９％となり，やはり逆比例の関係となることを示した。ガス放出率の絶対値は，以前のテストと比べ少なかったが，これは酸素含有率に関係していると考えられる。

（Ｋ６Ａ，Ｋ６Ｂの酸素含有率は５００ｐｐｍ以下。以前のテストでは１１００～４４００ ｐｐｍ）

・被覆管歪み量（△D／D）……最大のトータル歪み量（△D／D）はスミアー密度に直接関係している。燃料組成が（U，Pu）Cだけの場合と（U，Pu)$_2$C$_3$の含まれている場合を比較すると（U，Pu）Cだけの場合の方が△D／Dはやや大きい。

（Fig.2）

被覆管の密度測定から得られるスウェリング量は極めて少なかった。

K6B：0.05～0.08％（フルエンス ≈ 3.8～3.9×10^{22} n/cm^2
最高温度 ≈ 560～575℃）

K6A：0.33～0.38％（フルエンス ≈ 5.1～5.5×10^{22} n/cm^2
最　　度 ≈ 565～570℃）

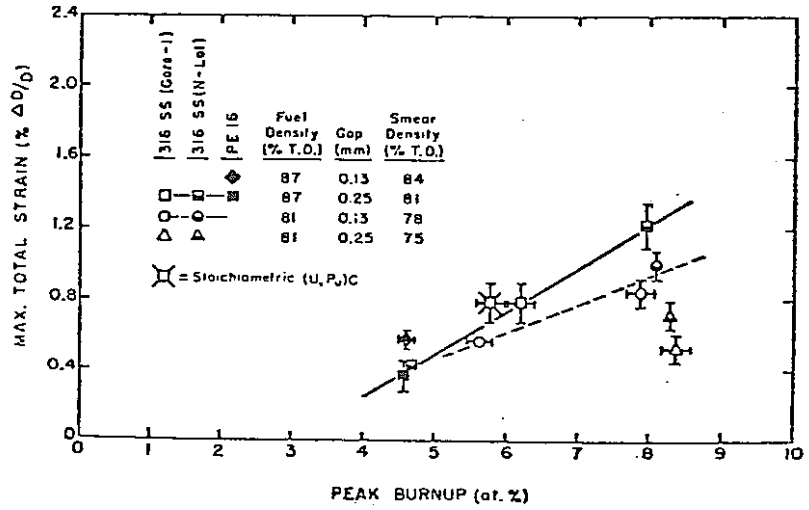

Fig. 2 Maximum cladding strain vs peak burnup for K6A, K6B, K7, and WSA-31 Series helium-bonded carbide fuel elements.

被覆管の直径増加は，大部分PCMIにより発生したもので，プロファイルメーター（Fig.3）からそれが一層明らかとなる。

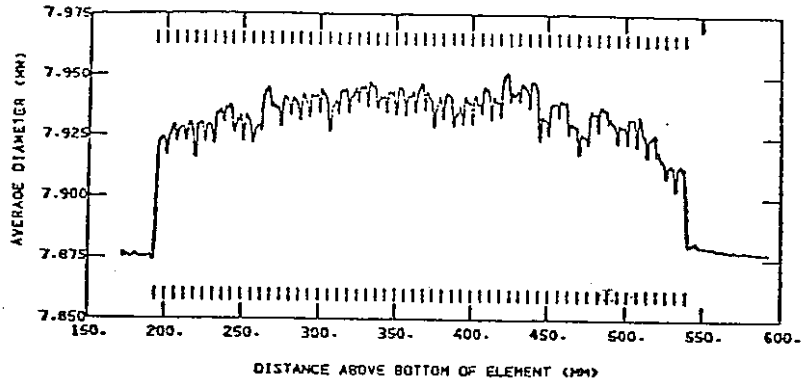

Fig. 3 Profilometry and fuel-pellet-interface positions for element K6A-52

・スタック長変化……M_2C_3が少ない方が，焼きしまり量が多く，スタック長の変化は少ない。

・FCCI …… 燃焼が進んでもFCCIはほとんど観察されない。M_2C_3を多く含んだ燃料では被覆管に炭化による硬化が見られる。（40μm位）

・被覆管の破損……WSA－31－17ピンで破損が発生。WSA－31－17は周辺ピンで，87%T.D.，0.13㎜ギャップで被覆管はNimonic PE16である。

破損は15㎜の長さで，燃料カラム中心位置より下方18㎜の所に位置し，ワイヤの真下である。ワイヤーは，その破損点では，隣接ピンに接触していた。

LIFE－3コードでは破損原因は明らかにできなかった。被覆管の折出物などから局所高温と関連付けられて破損原因の究明が進められている。

○オーバーパワートランジェント試験結果 ⑭

フレッシュなピン及び照射されたピン（燃焼度6.1，8.4 atom%）に対し，TREAT炉を用いてオーバーパワートランジェント試験を実施した。結果は，Heボンド，Naボンド（シュラウド付）のどちらの場合も，ギャップが極端に狭い場合を除き，一般にかなり高い健全性を示し，少なくとも酸化物燃料と同等レベルと評価して良いことが解った。

(3) 窒化物燃料 ⑫

○Naボンドピン

照射した何本かのピンに破損を生じたが，これらはいずれも，シュラウドなしで被覆管肉厚0.53㎜以下のピンである。

（照射後試験結果）

・ペレットスウェリング……半径方向で1.5%／atom%。半径方向の方が軸方向より25%程率が高い。燃焼度が6 atom%を越すと急にスウェリング率が増加する。

・被覆管歪み量（ΔD/D）……ピン直径増加は，PCMIでなく，被覆管のスウェリングによる。

・FCCI……FCCIは，まったく観察されない。また，被覆管の硬度変化も見られない。

・FPガス放出率……0.81～1.56%。放出率の高いのは，シュラウドなしのピン。

○Heボンドピン

線出力が高く（100KW/m以上），被覆管最高温度も高く（670～730℃）で，かつスミア密度の高いピンの場合のみ破損が見られる。それ以外では，8 atom%の燃焼度まで破損は生じていない。

（照射後試験結果）

・破損ピン……破損ピンは２本（Ｃ６－７，Ｃ７－２１）。破損は，コア中心付近で発生し，軸方向の小クラックであった。

残りの健全ピンを炉内に再装荷して，照射をさらに続けた時，さらに１本（Ｃ7－15）破損が発生した。

・被覆管歪み量（△Ｄ／Ｄ）……破損ピンは，いずれもスミア密度の高いピンで発生した。しかし，その外径変化は，最っとも少ないグループに属する。

プロファイルメトリーから，燃料カラムの境界で△Ｄ／Ｄが急に増加し，かつペレットの両端でリッジング現象が見られる。被覆直径変化が主にＰＣＭＩによることがこれから解かる。

燃焼度と△Ｄ／Ｄの関係は△Ｄ／Ｄ＝0.48％／atom％。（Fig.5）

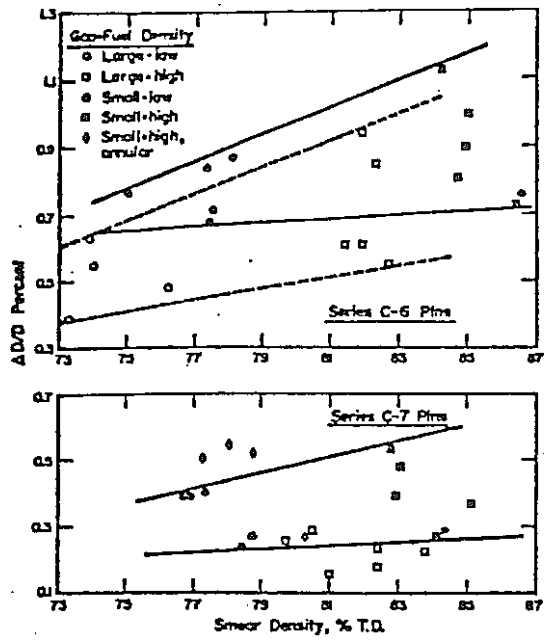

Figure 4 Helium-Bonded Fuel Element Diametral Expansions as a Function of Smear Density (* Failed Element)

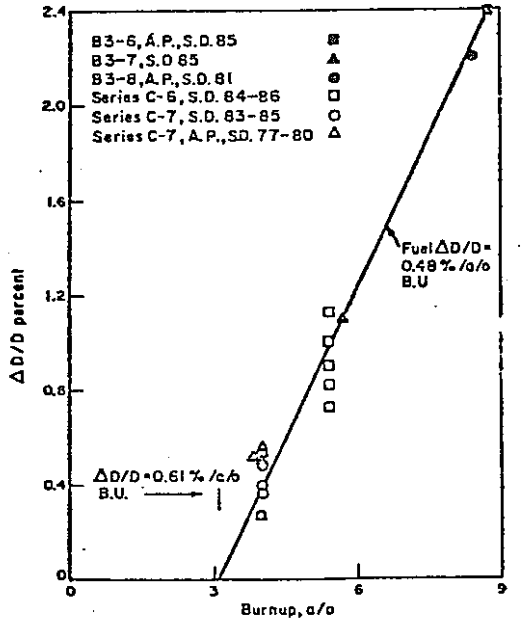

Figure 5 Helium-Bonded Fuel-Element Diametral Expansion is a Function of Burnup

附録－2

IRRADIATION PERFORMANCE OF MIXED OXIDE FUEL PINS
-JAPANESE EXPERIENCE
（混合酸化物燃料ピンの照射挙動）

K. Uematsu, Y. Ishida, J. Komatsu and T. Kawata

IRRADIATION PERFORMANCE OF MIXED OXIDE FUEL PINS - JAPANESE EXPERIENCE

K. Uematsu, Y. Ishida, J. Komatsu and T. Kawata

ABSTRACT

Within the frame of Japanese program of developing fast breeder reactors, the Power Reactor and Nuclear Fuel Corporation (PNC) has made intensive efforts in conducting irradiation testing of oxide fuel pins in foreign and domestic reactors. During the past ten years, a total of 155 fuel pins has been irradiated in both thermal and fast flux conditions.

This paper summarizes experiences obtained to date with respect to fuel pin behaviors including thermal performance, fuel dimensional changes, cladding deformations and fuel-cladding chemical interactions.

INTRODUCTION

The development of fast breeder reactors in Japan set forth in 1967 when the Government approved the construction of two fast reactors, the experimental reactor Joyo first and the prototype reactor Monju next, as key milestones leading to commercial LMFBR's. An intensive research and development work directed to these reactors was then initiated in widely spread technical areas.

The effort of fuel development has been primarily concentrated on mixed-oxide fuels clad with stainless steel because they were decided to be used in Joyo and Monju as the most promising candidate of fuel system for near-term LMFBR's. Irradiation testing plays a key role in the area of fuel system development and a total of 155 mixed-oxide fuel pins has been irradiated over the past ten years in foreign and domestic test reactors.

This paper outlines the present status of Japanese irradiation test program and reviews experiences on oxide fuel pin behaviors derived to date.

OUTLINES OF STEADY-STATE IRRADIATION TEST PROGRAM

Joyo Mk-I core fuel pin is fueled with 93.5 % T.D. mixed-oxide and

clad with 6.3 mm diameter x 0.35 mm wall thickness, 10 % cold worked type 316 stainless steel. Fuel subassemblies consist of 91 fuel pins spaced with spiral wires. The goal burnup of Mk-I core is 50,000 MWD/MTM which corresponds to the peak fluences of 7×10^{22} n/cm^2 ($E \geq 0.1$ MeV). Joyo Mk-I core is scheduled following two years operation to be modified into the core more suitable for conducting irradiation testing.

The primary feature of Monju fuel pin design is an adaptation of the fuel with lower density (~85 % T.D.) than in Joyo mainly from the necessity to accommodate fuel swelling at high burnups. The cold work of Monju fuel pin cladding is raised up to 20 % to improve swelling resistivity. The operation of Monju is aimed to achieve fuel burnup of 80,000 MWD/MTM in core average and the fast neutron fluences corresponding to the peak burnup accumulate up to 2.3×10^{23} n/cm^2.

The steady-state irradiation test program in Japan is scoped principally to prove sufficient performance capabilities of both type of fuel pins under anticipated conditions. Major portion of the tests has been and is being conducted in fast flux conditions to investigate the phenomena induced by the exposure to high energy neutrons. Thermal flux tests are also valuable to investigate fundamental or specific aspects of fuel pin behaviors. Thus the irradiation test program in PNC may be categorised as follows;

(1) Steady-state irradiation tests of Joyo type fuel in fast flux.

(2) Steady-state irradiation tests of Monju type fuel in fast flux.

(3) Thermal flux irradiation tests for basic fuel studies.

A total number of fuel pins irradiated to date has accumulated up to 155. Forty-six out of these pins were associated with the performance tests of reference Joyo Mk-I fuel pins. The highest burnup achieved in this category was 55,000 MWD/MTM which well exceeded the goal burnup of Joyo Mk-I core. The irradiation tests oriented to Joyo has completed except one experiment, Rapsodie PNC-10, which is designed to assess Joyo Mk-II fuel pin design. In Mk-II core, which is scheduled to follow Mk-I core after its operation for two years and is designed to have capabilities as a irradiation test facility, the diameter of driver fuel pins are reduced to 5.1 mm to improve neutron flux over 5×10^{15} n/cm^2·sec.

Current irradiation program is mostly orientated to the assessment of Monju type fuel pin design and irradiation has completed for 50 fuel pins so far. Reflecting the late start of Monju type cladding development, the 10 % cold worked cladding tubes developed for Joyo were used in the early phase of Monju fuel pin test program. The highest burnup attained in this phase of program is 128,000 MWD/MTM in Rapsodie PNC-4 (3) experiment.

The first experiment with 20% cold worked caldding is 34 fuel pin sub-assembly test, Rapsodie PNC-5 (1), which was disassembled for examination after reaching 59,000 MWD/MTM peak burnup. Three pins were selected and mounted into a capsule for further irradiation.

The burnup status of each fast flux experiment is summarized in Fig. 1.

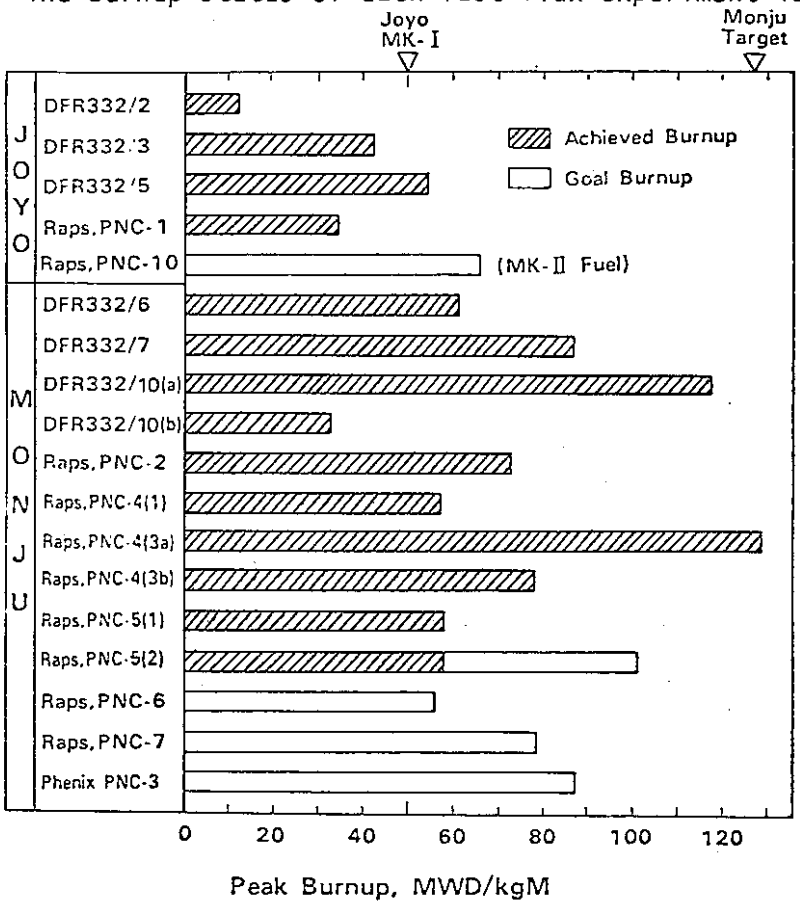

Fig. 1.

Burnup Status of PNC Stasdy-State Irradiation Test Program in Fast Flux

IRRADIATION BEHAVIORS OF MIXED OXIDE FUEL PINS

Thermal Performance

In the current design criteria for LMFBR, fuel melting is prohibited at any moment of steady-state operation which includes~15 % overpower conditions.

Fast flux irradiation tests conducted for Joyo type fuel pins covered the ranges of linear heat rating up to 510 W/cm maximum and the post-irradiation examinations disclosed no fuel melting in any of these tests.

Fuel melting was studied in GETR-T experiment where a total of eight fuel pins was subjected to overpower conditions. These fuel pins. with the fabrication parameters similar to those of Joyo, were preirradiated to the peak burnup of 18,000 MWD/MTM at mild operating power. Overpower experiments were performed with instrumented capsules in a thermal flux of GETR pool position and temperatures were monitered and controled to keep at the aimed pin rating. Metallographic examination revealed, among the pins where melting occurred, one pin overpowered to 880 W/cm had experienced typical incipient fuel melting. The power-to-melt directly determined from this experiment is, however, not prototypic to that in fast flux conditions and thermal analyses were necessary to correct this power to typical FBR conditions. The power-to-melt for Joyo type fuel was estimated by these analyses to be 611 ± 60 W/cm which is comparable within error band to the previously reported values.[1] These experiments proved the conservativeness in Joyo operating conditions.

Fuel restructuring is an important phenomenon which significantly contributes to the improvement of beginning-of-life fuel thermal performance. Several short-term irradiation experiments carried out in GETR and JMTR exhibited in general that the formation of center void in fuel approaches near-equilibrium state within range of a few hours to one day for the linear heat rating above 450 W/cm (in fast flux condition). On the contrary, the fuel with high density (~93 % T.D.) operated at the linear power below 400 W/cm only developed radial cracks and formed no appreciable size of center void after the irradiation for 300 days. Both the extent and the development rate of restructuring strongly depend on the operating power.

Thermal operating limit of Monju type fuel pins are predicted to be lowered to some extent due to the utilization of lower density fuels than in Joyo. Thus the programs are in progress to provide experimental data to characterize this limit and also to improve thermal analysis methods.

A significant improvement of thermal performance during the beginning phase of irradiation is also expected from the observation of rapid closure of fuel-cladding gap discussed later.

Fuel Length Stability

Fuel rod collapses due to the in-reactor densification of UO_2 fuel were experienced in several light water reactors (LWR's).[2] In fast reactors, however, densification in the form of fuel column shrinkage should present no crucial problems thanks to low coolant pressure, even though it is still

an unfavorable phenomenon if the amount of shrinkage is excessively large, The out-of-pile tests actually suggested the possibility of densification to some extent for some type of fuels, especially for such low density fuel as in Monju.

The changes of fuel column length were examined from X-ray radiographs or neutron radiographs. As shown in Fig. 2, a slight decrease in fuel column length was observed in several fuel pins with very low burnups but the magnitude of the reduction did not exceed 0.5 %. This initial tendency of fuel column length reduction is followed by the elongation at apparently constant growth rate of approximately 1 to 1.5 % per atom %. Data include those for both high and low density fuels but no difference in the tendancy of length change was recognized between two types of fuels. An apparently excess column elongation observed in some of fuel pins is attributed to a number of pellet separations (each clearance less than 0.5 mm). In conclusion, no problems in LMFBR fuel pins are forecasted from experimental observations relevant to densification.

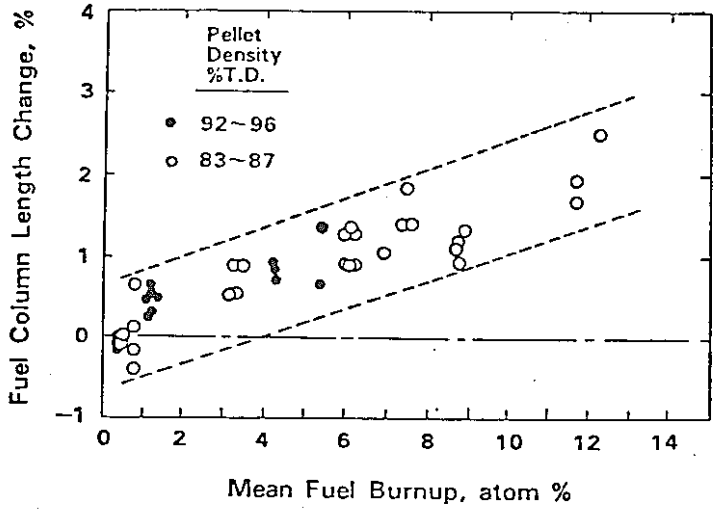

Fig. 2. Fuel Column Length Change with Burnup

Fuel-Cladding Gap Behavior

The post-irradiation fuel-cladding gap size is the subject to be carefully investigated in the irradiation tests because it is an essencial parameter which sensitively affects both thermal and mechanical behavior of oxide fuel pins.

Eight fuel pins were irradiated in JMTR for very short period (20 min. to 10 hours) to investigate early-in-life thermal behavior. The post-irradiation photomicrographs on those pins exhibited 5 to 50 % decrease in fuel-cladding gap width. This indicates a significant portion of gap

closure, which possibly leads to an improvement of fuel pin thermal characteristics, should occur during the first reactor start up/shut down if the linear power is reasonably high (>400 W/cm). It was indicated, as assumed in several analytical computer codes[3], the initial gap reduction was mainly caused by radial displacement of cracked pellets followed by partial healing.

Figure 3 illustrates the observed post-irradiation gas sizes as a function of local fuel burnup. Data, mostly gathered from the fuel pins irradiated in fast flux, were supplemented for very low burnup ranges with those from thermal reactor tests. A very rapid decrease of fuel-cladding gap width with burnup was observed in Fig. 3. The rate of gap closure appears to depend on fuel pin rating. This observation is consistent with the model proposed by Dutt et al[4].

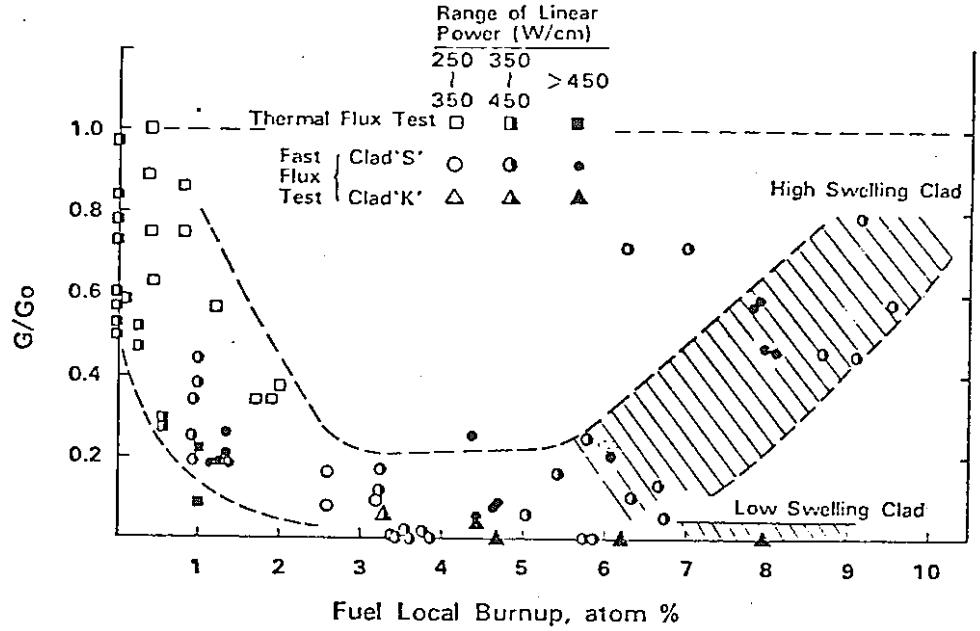

Fig. 3. Changes of Post-Irradiation Gap Width with Burnup

Note that data shown in Fig. 3 do not cover the cladding temperature range above 550°C because of the difficulty in gap size determination due to complex formation of reaction layers. The direct application of simple gap closure model, developed by Dutt et al. for instance, for such high temperature ranges (>550°C) seems to be inadequate and more careful insight is necessary in this area because the formation of reaction products between fuel-cladding interface is reported to influence the thermal-mechanical behavior of mixed oxide fuel pins at high burnup.[5]

The omen of gap reopening at high burnup was observed in some of fuel pins which eventually experienced large clad swelling, over 6 % in one of Rapsodie PNC-2 fuel pins for instance. This experiment also included the fuel pin with different lot of cladding which did show effectively no swelling at the same exposure. The gap remained closed in the latter fuel pin. Comparison of the extent of restructuring between two types of fuel pins suggested the temperature raise in the gap-opened fuel. This suggestion is further supported by the fact that the fission gas release rate was higher for this fuel pin. The results from the other pin suggested that gap reopening could be well suppressed by the utilization of cladding with improved swelling resistivity but will not eliminate the apprehensions of its occurrence in Monju where the fluences accumulate much faster than in small test reactors. Further investigations are required on the gap width changes at high exposure because it could give rise the problem in late-in-life thermal performance.

Fuel Pin Deformation

The data compilation on fuel pin geometrical changes plays an important role in identifying fuel pin integrity limit and also in establishing sufficient insight into the mechanical behavior of fuel pins. The maximum pin diametral strains measured in a series of DFR experiments are plotted against peak burnup in Fig. 4. Two types of fuel pins with different smear density were involved in this study and a significant reduction in pin diametral increases for low density fuel was found.

Along with diametral increases, the irradiation causes pin elongations. It is suggested by immersion density measurement that the length change is approximately consistent with the summation of cladding swelling along the length of fuel column (theoretically over the length of fuel pin, but the contribution from regions outside fissile column is practically negligible). This implies that the elongation of fuel pins due to strong pellet-cladding interaction as observed in some of LWR fuel rods is not likely to occur in LMFBR's. A slight discrepancy observed in some of fuel pins may attributed to swelling unisotropy.

Cladding inelastic strains, usually evaluated as total diametral strains minus one-third of volumetric swelling, are more direct indices for the wastage of fuel pin endurance capabilities. Since the pin length change devided by the length of fuel column ($\Delta L/Lf$) approximately represents the cladding swelling averaged over the latter length, the substraction of $\Delta L/Lf$ from mean diametral increase, which is again averaged over the length of fuel column, yields mean inelastic strain. Figure 5 illustrates the mean inelastic strains evaluated by this method. The results indicate there sxists an incubation period of burnup for inducing

inelastic strains. The threshold burnup above which the inelastic strains set in is approximately 4 atom %. It must be noted that this threshold burnup is consistent with the timing of completing gap closures (see Fig. 3).

Immersion density measurements on fuel-removed cladding specimens allow direct evaluation of local inelastic strains. Data compiled on fuel pins with 79 % smear density have indicated a strong dependence on irradiation temperatures as illustrated in Fig. 6, where the incubation of inelastic strain below 4 atom % burnup was seen again. Because the diametral strains in plenum region observed to data were always negligible, the accumulation of fission gas pressure is not responsible for these mechanical deformation. Therefore, these inelastic strains are considered

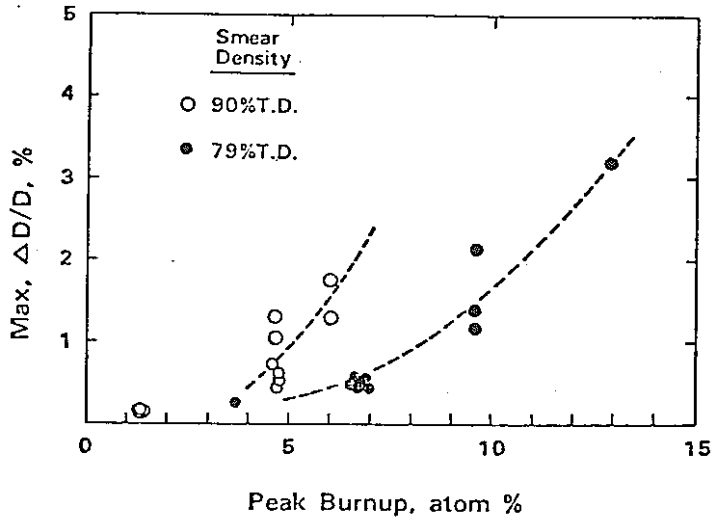

Fig. 4 Pin Diametral Increase with Burnup

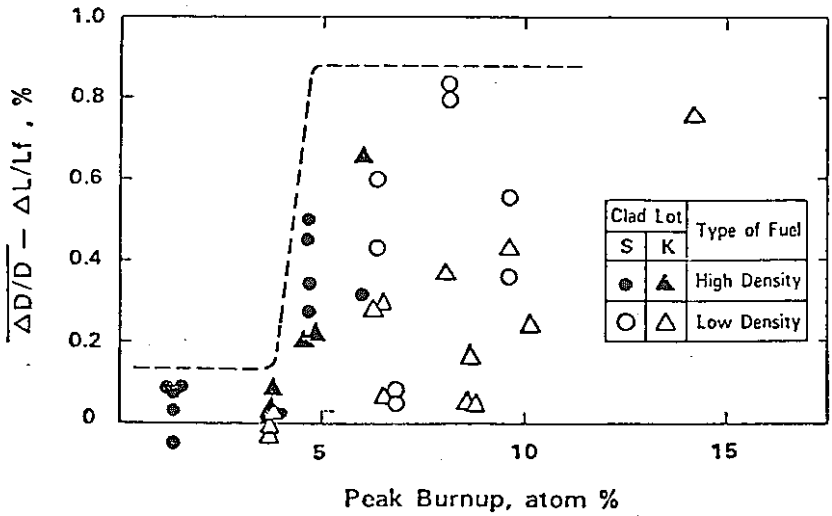

Fig. 5. Mean Inelastic Strain V.S. Burnup

to be caused by fuel-cladding mechanical interaction. This explanation is further justified by the comparison of inelastic strains between fuel pins with varied smear densities. A significant decrease in cladding inelastic strains of fuel pins having smear density of 79 % T.D. compared with those having 90 % smear density was found in Fig. 7.

A series of irradiation tests for Monju type fuel have been conducted in Rapsodie. The results revealed an obviously different behavior between the fuel pins whose cladding tubes were taken from separete two lots. One of the fuel pins clad with lot 'K' tubing successfully achieved originally aimed burnup of 14 atom % with the maximum diametral increase about 2.4 % , while other fuel pins with lot 'S' tubings caused, at approximately 8 atom % burnup, excess bulgings ($\sim$3.7 % $\Delta D/D$) which resulted in a rupture of one pin. Immersion density measurement disclosed the maximum swelling of 6.7 % at fluences of 6 x 10^{22} n/cm^2 ($E \geqq 0$, 1MeV) for lot 'S' cladding.

Cladding inelastic strain was also found to be significant in this fuel pin and reached 1.2 % in maximum. Swelling and inelastic strains observed in the other lot of cladding were, in contrast, very small at the same fluences. Because of the nature of typical steady-state irradiation, major components of inelastic strains observed in these tests are not likely to have been caused by plastic deformation but they appear to have resulted from creep strains, where irradiation-induced creep have presumably played an important role. Differences disclosed between two cladding lots have suggested a strong correlation between creep under-irradiation and swelling.

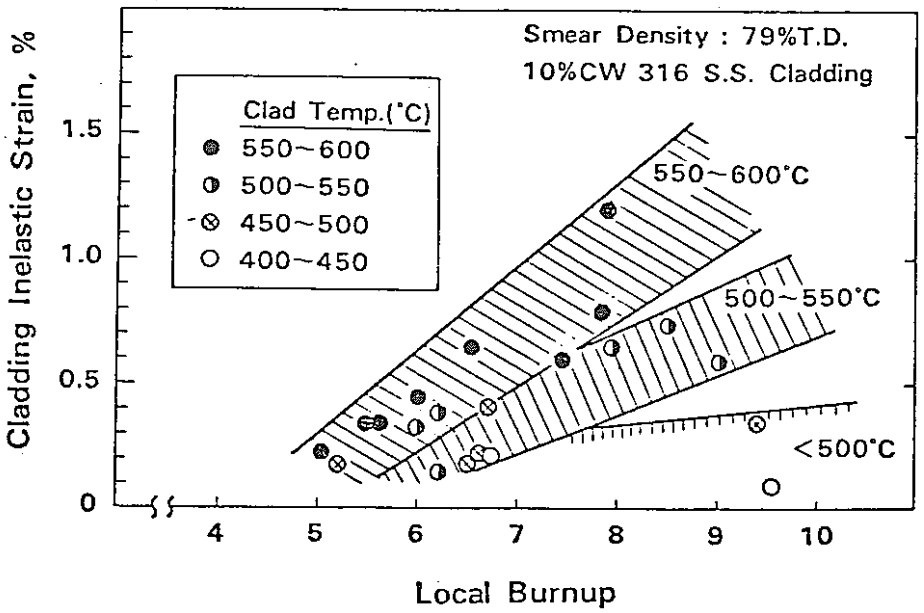

Fig. 6 Increase of Cladding Inelastic Strain with Fuel Burnup

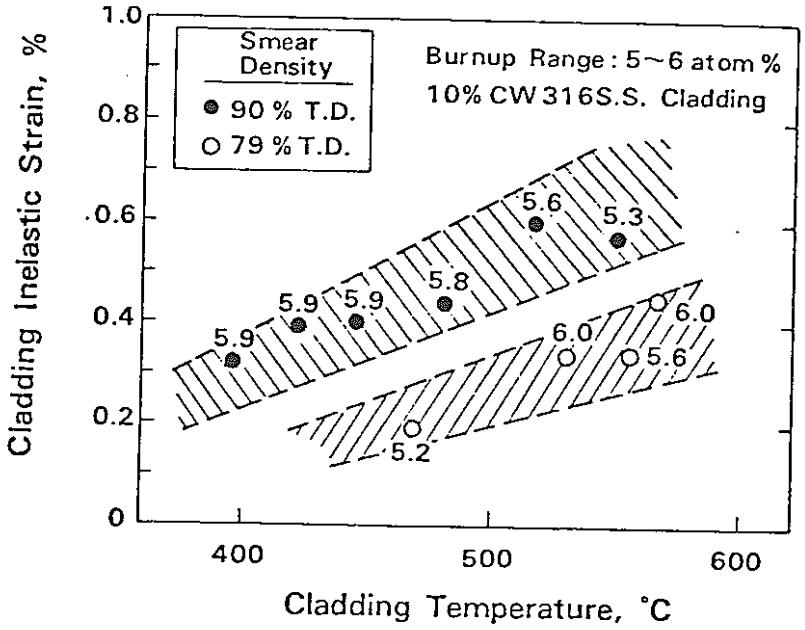

Fig. 7. Effect of Fuel smear Density on Cladding Inelastic Strain

Differences between these two cladding lots were only in the minor chemical constituents and also in some portion of fabrication processes. Thus the experiment have eventually pointed out the importance of these factors in characterizing behaviors of cladding materials under irradiation.

Fuel-Cladding Chemical Interaction

The effect of fuel-cladding chemical interaction (FCCI) is counted in fuel pin design as a reduction of effective cladding thickness which directly reduces the load-bearing capability of fuel pin cladding. Figure 8 summarizes the data on the maximum depth of attack measured from PNC experiments where the oxygen to metal ratios range from 1.98 to 2.00. No significant burnup dependence is seen for the burnup range above 4 atom % in this limited data set. The maximum depth observed was generally bellow 80 μm except one data point. Data included those for Joyo and Monju fuels and no difference in FCCI characteristics was observed between these two types of fuels. No cladding attack was observed for the range of cladding inside surface temperatures below 500°C. For the temperature range above 500°C, the trend of increase in attack depth with increasing temperature is seen in the bulk of data set. Axial locations of the maximum attack depth for individual fuel pins, however, were not necessary to be at the hottest end but appeared to distribute occationally to cooler positions. These observations call for full understanding on the axial transport behavior of fission products.[6] Electron microprobe analyses have

shown the important role of Cs, Te and other fission products in the formation of cladding corrosion.

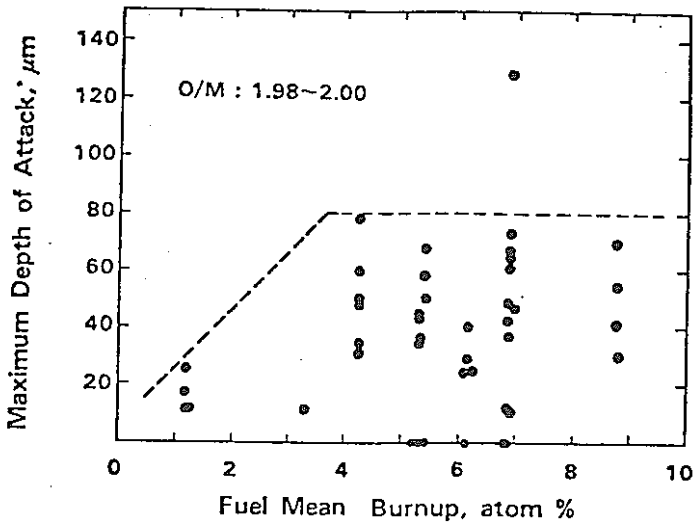

Fig. 8. Maximum Depth of Cladding Attack V.S. Burnup

Cladding Breach Experiences

Several types of cladding breaches have been observed in the steady-state irradiation tests to date.

One of the fuel pins in DFR 332/5 experiment failed from localized overheating caused by gas bubble attachment, which is often observed in DFR. A typical 'tear-stain' mark was observed in the vicinity of the cladding ruputure. A significant reduction of cladding microhardness localized in the area of this mark was observed, which convlusively proved the occurrence of overheating. Sodium ingress caused secondary cracks in the lower portion of this fuel pin.

The irradiation of Rapsodie PNC-2 experiment was interrupted at 73,000 MWD/MTM because of the detection of fission gas leak. A cladding rupture occurred in one of four fuel pins at the location 7 cm above core midplane. This rupture was associated with large diametral increase (3.7 % max.) and pin twisting in the upper half of fissile column region. The cause of this failure is not fully understood yet but an anomalous increase of temperature is suspected to have occurred locally from the gradual reduction of pin-to-capsule-wall clearance by increasing pin twisting. The strong twisting of this fuel pin must be attributed to very rapid swelling and irradiation creep rates in the specific lot of cladding used.

Therefore, cladding breaches described above are classified as those caused by specific anomalities. In other words, those breaches were not resulted from typical wear of cladding endurance limit.

Two fuel pins from DFR 332/7 experiment were reirradiated after the non-destructive examination at originally aimed burnup of 87,000 MWD/MTM to investigate the actual endurance limit of these pins. Cladding breaches occurred in both fuel pins during the second run from re-insersion into the core of DFR. Only non-destructive examination data are available at present time but the appearance of breaches are considered to be that of endurance limit failures. Analyses to correlate these breaches to cummulative life fraction damage are in progress.

Breaches experienced by PNC are only for 10 % cold-worked cladding and no appreciable effect from the breach was identified on the neighboring fuel pins in any of those cases.

CONCLUSION

Experiences related to the irradiation testing of FBR oxide fuel in Japan over the past ten years were reviewed.

A series of tests were conducted for Joyo type fuel pins and the results showed their satisfactory behaviors and stabilities up to the aimed burnup in Joyo. Ongoing programs are mostly those for the assessment of Monju type fuel pins.

The high fluence tests evidently indicate that the operating capability of FBR fuel pins is dependent to a large extent on the performance of cladding materials used. From the limited experiences obtained to data, it is foreseen that the primary factor to limit fuel pin lifetime would be the dimensional distortion caused by swelling and irradiation creep in cladding under high exposures rather than typical wear of clad material endurance capabilities. Therefore, an emphasis in the fuels and materials development must be placed on the development of cladding (and duct) materials with improved resistivities to swelling and creep under irradiation.

Joyo is currently operating at 50MW and the post-irradiation examination on the first fuel subassembly was recently initiated. The post-irradiation examination plan for Joyo is programmed to produce data on oxide pin and subassembly behaviors properly distributed on the variable irradiation conditions achievable in Joyo Mk-I core. A statistically meaningful number of data are expected to be produced. Analyses on those

massive and systematically distributed data will significantly contribute to improving phenomenological understanding of oxide fuel pin behaviors and also to reducing uncertainties in a quantitative interpretation or prediction of those behaviors and operating limits. In addition, a numerous number of irradiation experiments in the wide range of fuels and materials are planned in future utilizing Joyo Mk-II core as a test facility.

REFERENCES

1. R.D. Leggett, E.O. Ballard, R.B. Baker, G.R. horn and D.S. Dutt, "Linear Heat Rating for Incipient Fuel Melting in UO_2-PuO_2 Fuel," Trans. Am. Nucl. Soc., 15, 752-753, (November 1972).

2. Y. Mishima, et al., "Performance of Light Water Reactor Fuel and Reactor Safety," (in Japanese), Nippon Genshiryoku Gakkai-shi, 18, 14-23, (January 1976).

3. M. Ishida, M. Sakagami and S. Kikuchi, "An Analysis of Mechanical Interaction Between Fuel Pellets and Cladding in LMFBR Fuel Pins," This Meeting.

4. D.S. Dutt, R.B. Baker and S.A. Chastain, "Modeling of the Fuel Cladding Post-irradiation Gap in Mixed-Oxide Fuel Pins," Trans. Am. Nucl. Soc., 17, 175, (November 1973).

5. R.A. Darneskey, "Effects of Local Cesium Concentrations on Mixed-Oxide Fuel Behavior,"Trans. Am. Nucl. Soc., 27, 229-231, (November 1977)

6. K. Uematsu, Y. Ishida, J. Komatsu and T. Kawata, "Migration Behavior of Cesium in Mixed Oxide Fuel Pins," This Meeting.

附録－3

MIGRATION BEHAVIOR OF CESIUM IN MIXED OXIDE FUEL PINS
（混合酸化物燃料ピンにおけるC_2の移行）

K. Uematsu, Y. Ishida, J. Komatsu and T. Kawata

MIGRATION BEHAVIOR OF CESIUM IN MIXED OXIDE FUEL PINS

K. Uematsu, Y. Ishida, J. Komatsu and T. Kawata

INTRODUCTION

Mixed oxide fuel pins irradiated in fast reactors and thermal reactors reveal the migration of fission products. The migration of fission products may have significant influence on fuel performance. Then the fission products behaviors are the subjects of great interest to the fuel designer and chemist. It is the objective of this paper to summarize the observations of characteristic behavior of cesium and effects of migration on the performance of fuel pins irradiated so far.

For the development of the fast breader reactor JOYO and MONJU, a total of one hundred fifty five fuel pins has been irradiated in Dounreay Fast Reactor (DFR), RAPSODIE, General Electric Testing Reactor (JMTR). The fuel desities of these pins were ranged from 95%TD to 85%TD and oxygen to metal ratios were ranged from 1.98 to 2.00. The fuel pin cladding was 6.3mm OD, 0.35mm in thickness and 10% cold worked Type 316 stainless steel. The irradiation was carried out up to the burnup of 14 at.% with a peak linear power of 400~500 W/cm.

During the post irradiation examinations of these pins, the migration behaviors of fission products have been examined by neutron radiography, gamma spectrometry, optical metallography and microprobe analysis. Some of pins revealed the migration of cesium both radially and axially to the cooler region of the fuel by a vaporization-condensation process. This fission product sometimes induced fuel-cladding chemical interactions and local cladding strain. These phenomena have been carefully observed.

In this paper, some of the experimental results is presented. Table I shows the outline of the fuel pins and irradiation conditions in this experiments.

Table I. Pin Design Parameters and Irradiation Conditions

Experiments Designation	Number of Pins	Pin		Fuel				Cladding		Irradiation Conditions		
		Length mm	Diameter mm	Pu/(U+Pu)	O/M	Density %TD	Form	Material	Conditions	Peak Power W/cm	Peak Burnup at.%	Peak Midwall Cladding Temp. °C
DFR 332/2	6	266	6.3	0.18	1.880	95.8	Pellet	316SS	6%CW 18%CW	510	1.2	640
DFR 332/7	3	550	6.3	0.20	1.984	84–85	Pellet	316SS	10%CW	420	9.6	650
GETR-T	12	159	6.3	0.2	1.991	91.3	Pellet	316SS	10%CW	520 810/850* 990/1080	2.0	550 560/610* 650/730

*Over Power Test after Steady State Irradiation

MIGRATION CHARACTERISTICS

Axial Migration

One of three pins, which were irradiated in DFR at a peak linear power of 420 W/cm with midwall cladding temperature of 650°C to a peak burnup of 9.6 at. %, was examined in detail. In this experiment, DFR 332/7, three fuel pins were contained in a capsule. The fuel density and oxygen to metal ratio were 85% of theoretical and 1.984, respectively. The design parameters and irradiation conditions are shown in Table I.

Axial gamma ray scanning of this pin revealed the strong cesium peaks at the top and bottom interface between fuel and UO_2 insulator pellets. In addition, a cesium peak was also observed at the one fourth of the fuel column height from the bottom as shown in Fig. 1.

Gamma ray scanning of the longitudinal cross section of this pin at the interface of fuel/UO_2 insulator pellets ahowed that cesium was accumulated at interface for the top side, but not for the bottom side as shown in Fig. 2. Usually, cesium was accumulated at the interface between fuel and UO_2 insulator, not interior of UO_2 within the oxygen to metal ratio of 1.98 to 2.00. While at the bottom interface, cesium was observed interior of UO_2 insulator pellet. Considering the no oxygen to uranium ratio changes in an insulator pellet, this should have resulted from the higher

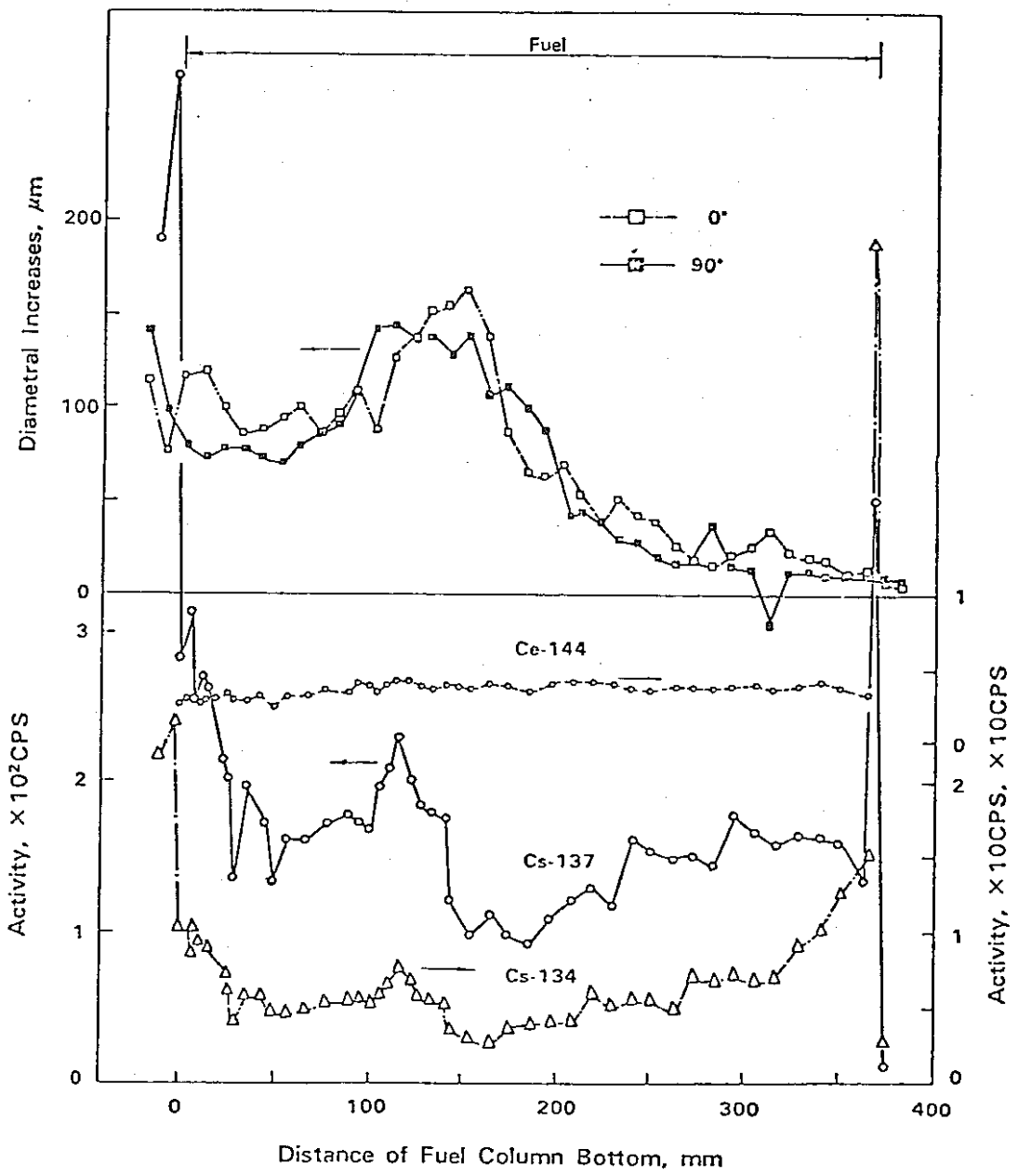

Fig. 1. Pin Diametral Increases and Axial Distribution of Cesium in $(U_{0.8}\ Pu_{0.2})\ O_2$ Fuel, Pin No. 1, DFR 332/7, Burnup 9.6 at.%, Power 420 W/cm

temperature of the bottom UO_2 insulator pellet because it is located at the outlet side of coolant. Then it is considered that cesium migrated to the interior and cooler region of UO_2 insulator pellet.

Form this and other experiments, it was observed that the cesium peaks within the fuel column are usually a few for the low burnup and low power pins, and are likely to be associated with the high burnup and high power fuel pins. And it has a tendency that the higher the power, the more the irregular distribution of cesium is observed within the fuel column. For the low burnup and low power pins, cesium tends to accumulate at the interface of fuel/UO_2 insulator pellets. Sometimes the local accumulation is also observed at pellet to pellet gaps.

The metallographic examination showed that the top and bottom fuel/insulator interface were usually desified at central part and several cracks or fragmentation were observed in UO_2 insulator pellets. A porous gray phase reaction products were sometimes observed in this zone. The alpha autoradiography showed that this gray phase was depleted in plutonium.

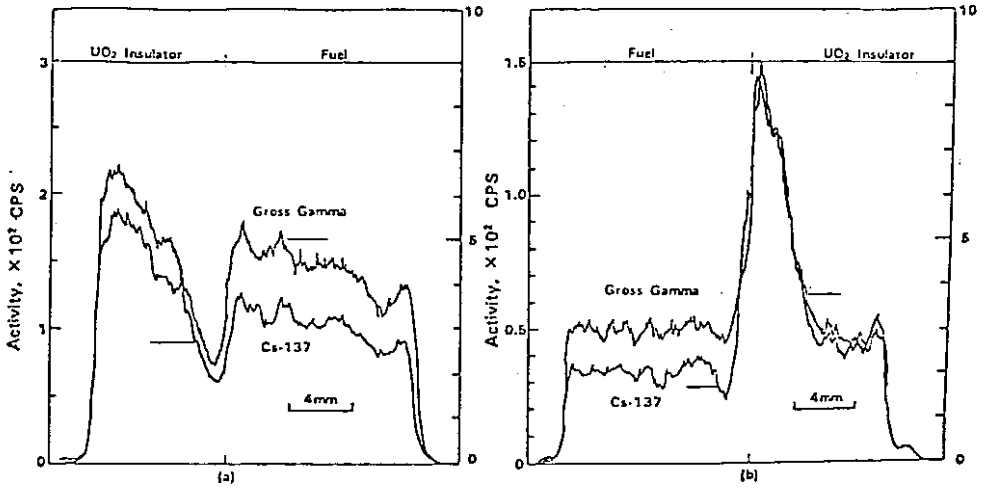

Fis. 2. Cesium Accumulation at Fuel/UO_2 Insulator Interface (a) Bottom Insulator Interface, (b) Top Insulator Interface Pin No. 1, DFR 332/7, Burnup 9.6 at.%, Power 420 W/cm

Radial Migration

Radial cesium migration was also observed by gamma ray scanning, microsampling analysis and microprobe analysis. The data from DFR 332/7 experiment are shown in Fig. 3(a). Cesium was accumulated at the gap between fuel and cladding. The cesium redistributions in the fuel obtained from the microdrilling samples in DFR 332/2 experiment are shown in Fig. 3(b). This specimen was irradiated in the DFR to the burnup of 1.2 at.% with the liner power of 510 W/cm as shown in Table 1. Cesium migrate toward the outer surface, while cerium, zirconium and niobium are almost evenly distributed in the fuel.

Microprobe analysis indicated that cesium, iodine, tellurium, barium and palladium are concentrated at the fuel cladding interface region. Cesium was usually associated with uranium and no plutonium was observed in this region. The gray phase in the fuel may be resulted in UO_2-cesium reaction products as other investigator pointed out.[1,2]

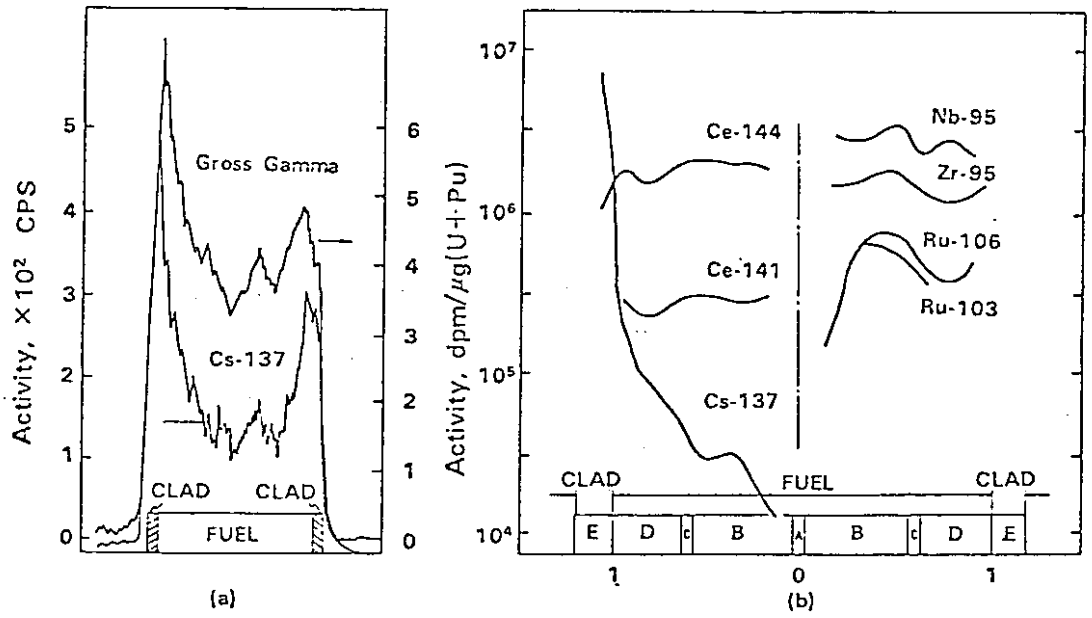

Fig. 3. Radial Migration of Cesium in $(U_{0.8}\ Pu_{0.2})\ O_2$ Fuel
(a) Gamma Spectrometry, Pin No.1, DFR 332/7, Burnup 9.6 at.%, Power 420 W/cm
(b) Microsampling Analysis, Pin No.5, DFR 332/2, Burnup 1.2 at.%, Power 510 W/cm
A. Central Void, B. Columnar Grain Region, C. Equiaxed Grain Region, D. Unrestructuring Region, E. Cladding

EFFECTS OF MIGRATION

The radial and axialimigration of cesium are known to affect the local cladding strain[3,4] and fuel-cladding chemical interactions.[5]

Local Cladding Strain

The local accumulation of cesium are compared with the data of local cladding strain obtained from the profilometry of fuel pins.

Some of fuel pins in GETR-T experiment, which was irradiated in GETR, revealed the local cladding strain at cesium peaks. The design parameters of this fuel pins are shown in Table 1. The fuel density and oxygen to metal ratio were 91.3 % of theoretical and 1.991, respectively.

In this experiment, twelve fuel pins were irradiated in an epithermal and fast flux enviroment by using a cadmium flux filter. Irradiation was carried out at the average peak linear power of about 440 W/cm with the midwall cladding temperature of 480°C to a peak burnup of 2 at.%.

After the steady state irradiation, eight fuel pins were selected and divided into four pairs of two pins. Each pair of axially connected fuel pins was reirradiated for twenty four hours at different four power levels ranged from 800 to 1000 W/cm, respectively. Some of pins was melted at high power.

After the steady state irradiation, the local cladding strain associated with the cesium peaks was not observed. However, after the overpower irradiations, the predominant cesium accumulation was observed within the fuel column and at fuel/UO_2 insulator pellet interface. These cesium peaks are associated with the local cladding strain as shown in Fig. 4. These strong correlations may be resulted from the high power and higher oxygen to metal ratio in this experiment. The internal cladding attack was not observed in this region.

From the microprobe analysis data showing a cesium usually associated with uranium, the local cladding strain may be caused by a volume increase associated with the formation of cesium uranates. However, the effects of the UO_2-cesium reaction products on fuel restructuring and fuel-cladding gap closing could not be defined in these experiments.

In DFR and RAPSODIE experiments, it was difficult to find the strong correlations between cesium accumulation and local cladding strain. Especially, it is difficult for high burnup pins to find strong correlations because of the cladding swelling and creep contribution to the deformation.

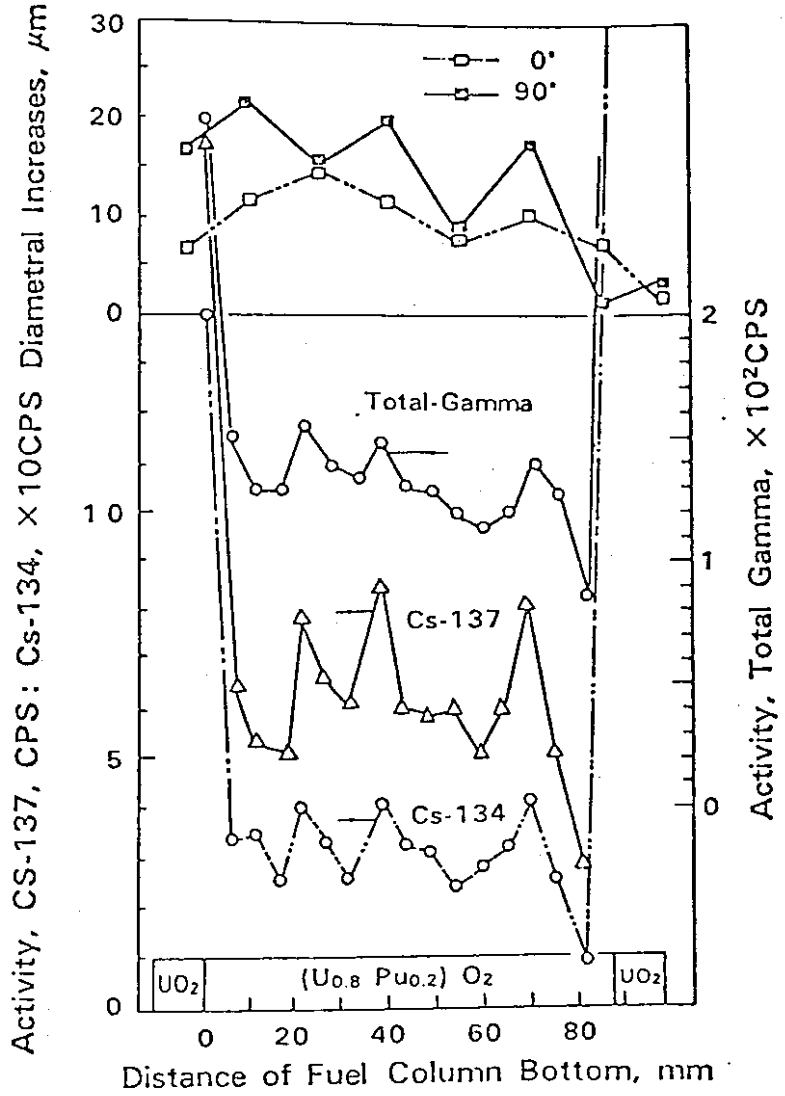

Fig. 4. Local Cladding Strain and Cesium Peaks in the Fuel Column, Pin No. 21, GETR-T, Burnup 2 at.%, Power 880 W/cm

From these experiments, the local cladding strain associated with cesium peaks appears to be influenced by the high burnup and high power. The oxygen to metal ratio has also significant effects on these phenomena.

Fuel-Cladding Chemical Interactions

In addition to local cladding strain, cesium migration also influences the fuel cladding chemical interactions above the temperature of around 500°C. The results of microprobe analysis indicate that cesium, iodine, and tellurium significantly contribute to this interactions.

SUMMARY AND CONCLUSIONS

Migration behaviors of cesium have been examined for the fast reactor mixed oxide fuel pins. Cesium migrate radially and axially to the cooler region of fuel pins.

Axial accumulation of cesium is observed at the interface of fuel/UO_2 insulator pellets and pellet to pellet gaps. For high burnup and high power pins, cesium accumulation are sometimes observed within the fuel column. And it appears to increase the irregular redistributions of cesium within the fuel column with increasing the burnup and power.

It is often observed a secondary gray phase at the fuel/UO_2 insulator interface and fuel cladding gaps. Microprobe analysis revealed the presence of uranium, cesium, iodine, tellurium and barium and no plutonium in this reaction zone. Thus the gray phase may be formed by UO_2-cesium reactions.

These local cesium accumulations sometimes induced the cladding strain at fuel/UO_2 insulator interface and within the fuel column. The strain appears to be resulted from the volume increase of UO_2-cesium reaction products.

The cesium accumulation is influenced by oxygen to metal ratio and temperature gradients. However, these local accumulation of cesium does not seem to limit the fuel performance.

REFERENCES

1. I. Johnson and C.E. Johnson, "Migration of Cesium and Molybdenum in Irradiated Oxide Fuels," Thermodynamics of Nuclear Materials 1974 (Proc. Symp. Vienna, 1974), 1, IAEA, Vienna, 99, 1975

2. L.A. Neimark, J.D.B. Lambert, W.F. Murphy and C.W. Renfro, "Performance of Mixed-Oxide Fuel Elements to 11 at.% Burnup," Nucl. Technol., 16, 75, 1972

3. R.A. Karnesky, R.D. Loggett, S.A. Chastain and J.W. Weber, "Cesium Migration in Mixed-Oxide Fuel Pins," Trans. Am. Nucl. Soc., 22, 229, 1975

4. R.A. Karnesky, "Effects of Local Cesium Concentrations on Mixed-Oxide Fuel Behavior," Trans. Am. Nucl. Soc., 27, 229, 1977

5. R.W. Ohse and M. Schlechter, "The Role of Cesium in Chemical Interaction of Austenitic Stainless Steels with Uranium Plutonium Oxide Fuels," EUR 4893 e, Aug. 1972